Local and global gravitational aspects of domain wall space-times

Mirjam Cvetič,* Stephen Griffies,† and Harald H. Soleng‡
Department of Physics, University of Pennsylvania, 209 South 33rd Street, Philadelphia, Pennsylvania 19104-6396
(Received 14 May 1993)

Local and global gravitational effects induced by eternal vacuum domain walls are studied. We concentrate on thin walls between nonequal and nonpositive cosmological constants on each side of the wall. The assumption of homogeneity, isotropy, and geodesic completeness of the space-time intrinsic to the wall as described in the comoving coordinate system and the constraint that the same symmetries hold in hypersurfaces parallel to the wall yield a general *Ansatz* for the line element of space-time. We restrict the problem further by demanding that the wall's surface energy density, σ, is positive and by requiring that the infinitely thin wall represents a thin-wall limit of a kinklike scalar field configuration. These vacuum domain walls fall in three classes depending on the value of their σ: (1) extreme walls with $\sigma = \sigma_{\rm ext}$ are planar, static walls corresponding to supersymmetric configurations, (2) nonextreme walls with $\sigma = \sigma_{\rm non} > \sigma_{\rm ext}$ correspond to expanding bubbles with observers on either side of the wall being *inside* the bubble, and (3) ultraextreme walls with $\sigma = \sigma_{\rm ultra} < \sigma_{\rm ext}$ represent the bubbles of false vacuum decay. On the sides with less negative cosmological constant, the extreme, nonextreme, and ultraextreme walls exhibit no, repulsive, and attractive effective "gravitational forces," respectively. These "gravitational forces" are global effects not caused by local curvature. Since the nonextreme wall encloses observers on both sides, the supersymmetric system has the lowest gravitational mass accessible to outside observers. It is conjectured that similar positive mass protection occurs in all physical systems and that no finite negative mass object can exist inside the universe. We also discuss the global space-time structure of these singularity-free space-times and point out intriguing analogies with the causal structure of black holes.

PACS number(s): 04.20.Jb, 98.80.Cq

I. INTRODUCTION

Domain walls are surfaces interpolating between separate vacua with different vacuum expectation values of some scalar field(s). Such a domain structure can form by the Kibble [1,2] mechanism whereby different regions of a hot universe cool into different isolated minima of the matter potential. Domain walls [2] can also form as the boundary of a (true) vacuum bubble created by the quantum tunneling process of false vacuum decay [3]. Additionally, the universe could be born through a quantum tunneling process from nothing [4–6] into different domains with walls in between.

The equivalence between mass and energy in relativistic physics implies that kinetic energy in the form of pressure also contributes to the gravitational mass density. Accordingly, a negative pressure, that is, a positive tension, reduces the effective Tolman mass [7] (i.e., the gravitational mass) of a system. Domain walls are vacuumlike hypersurfaces where the positive tension equals the mass density [2], thus ensuring that their energy-momentum tensor is boost invariant in the directions parallel to the wall. Taking into account the repulsive gravitational effect of positive tension [8], a domain wall is by itself a source of repulsive gravity [2,9], i.e., a system with negative effective gravitational mass. However, a bubble of anti-de Sitter vacuum (AdS_4) which has negative energy density and positive pressure, is a source of *attractive* gravity; it has a positive effective gravitational mass. If such a bubble is embedded in a Minkowski (M_4) space-time, the attractive effect of AdS_4, caused by its positive effective gravitational mass, could be undercompensated by the domain wall, which has negative effective gravitational mass. Inertial observers exterior to this object would find that the wall separating the two vacua accelerates toward them. Alternatively, it would *a priori* be possible that the effective gravitational mass of the domain wall could be negative enough to render the total gravitational mass of the system negative. Then the result would be a system of total *negative* gravitational mass [10–12], and observers on the side with a less negative cosmological constant would also be repelled from the wall.

It has been shown that *"under very general assumptions, no static nonsingular solution ... exists for the gravitational field of an uniformly planar matter distri-*

*Electronic address: CVETIC@cvetic.hep.upenn.edu
†Present address: Geophysical Fluid Dynamics Lab, Princeton University, Forrestal Campus, US Route 1, P.O. Box 308, Princeton, NJ 08542. Electronic address: SMG@gfdl.gov
‡On leave from the University of Oslo, Norway. Present address: NORDITA, Blegdamsvej 17, DK-Copenhagen 2100 Ø, Denmark.
Electronic address: HARALD@norsci3.nordita.dk or SOLENG@vuoep6.uio.no

bution" [13]. However, if the energy density of the adjacent vacuum is allowed to be negative, this result can be avoided. Namely, in this case the positive effective gravitational mass density of AdS_4 can precisely cancel the negative effective gravitational mass density of a domain wall. Hence, there do exist nonsingular solutions of Einstein's field equations for static, planar walls adjacent to AdS_4 [14–16]. Moreover, these solutions are realized as *supersymmetric* bosonic field configurations [15]. In Ref. [17] a classification of the possible supersymmetric walls has been given, and the global structure of the space-times induced by these walls has been explored in Refs. [18–20]. Supersymmetric walls adjacent to Minkowski space are of particular interest. The two vacua separated by these walls are *degenerate* in the sense that semiclassical tunneling between them is absolutely suppressed [21]. The exact cancellation [18] of the gravitational field of the supersymmetric—hereafter called *extreme*—domain wall and the negative vacuum energy of AdS_4 makes it possible for an observer to be arbitrarily close to such an infinite planar domain wall without feeling any gravitational effects. For this reason the wall can be viewed as a perfect shield for the gravitational field produced by the AdS_4 vacuum.

As the previous discussion indicates, the effects of an AdS_4 region on the local and global space-time properties of domain wall systems are significant. It is of interest to systematically investigate the space-times of domain walls separating regions of nonpositive cosmological constant in Einstein's theory of gravitation. This study is motivated in part also from the desire to make a connection of the extreme walls studied in Refs. [15–19] in the context of $N = 1$ supergravity to more general nonsupersymmetric configurations. We also bear in mind that there are many reasons for believing the effective theory describing low energy modes of the superstring is four dimensional $N = 1$ supergravity (see, for example, Ref. [22] for further discussion). The energy densities of supersymmetric vacua are strictly nonpositive, and thus they induce AdS_4 or M_4 space-times. Upon breaking supersymmetry, the vacua can have a negative, zero, or positive cosmological constant.

We present a study of the local and global properties of the space-times induced by vacuum domain walls between vacua of arbitrary cosmological constant. We are primarily concerned with the domain walls between vacua of nonpositive cosmological constants. These walls may be classified according to their energy-density [23]. The nonextreme domain wall configurations are defined as those with energy density greater than the corresponding extreme wall ($\sigma_{\rm non} > \sigma_{\rm ext}$), and the ultraextreme domain walls have a smaller surface energy density ($\sigma_{\rm ultra} < \sigma_{\rm ext}$) [23]. We start with the *Ansatz* that the gravitational field inherits the boost symmetry of the source, and we demand geodesic completeness of the space-time intrinsic to the wall as described in the comoving coordinate system, but we assume nothing about the topology of the (2+1)-dimensional space-times parallel to the surface of the domain wall. It turns out that non- and ultraextreme walls are nonstatic spherical bubbles. Ultraextreme solutions result in an expanding *ultraextreme bubble* which accelerates toward all timelike outside observers. This is the tunneling bubble [24] of false vacuum decay [3,25]. Solutions with energy density $\sigma = \sigma_{\rm non} > \sigma_{\rm ext}$ overcompensate the attractive gravity of the inside by having the energy density larger than the one of the extreme wall; those are objects with negative effective Tolman mass. This does, however, not yield a negative mass object inside our universe. Instead, in the case of vacuum domain wall bubbles, gravity warps space-time so that *both* sides are on the inside of the nonextreme bubble. Hence, nature protects itself against the possibility of objects with negative total gravitational mass by using topology to put all observers on the inside. This example leads to the conjecture that in analogy with cosmic censorship preventing naked singularities, there is also a cosmic positive mass protection. Note that these nonextreme walls, which are characterized by energy densities higher than that of the tunneling bubble, are examples of configurations for which supersymmetry provides a lower bound for the energy density. Bounds of this type have also been found in the black hole context [26,27]. On the other hand, the ultraextreme solutions with energy density $\sigma = \sigma_{\rm ultra} < \sigma_{\rm ext}$ correspond to objects of positive effective mass. Timelike observers on the side with the largest cosmological constant—observers in the false vacuum—will inevitably be hit by the inflating bubble. As seen by inertial observers in the Minkowski space, the fact that they are hit by the ultraextreme tunneling bubble can be understood as a purely kinematic effect with no connection to gravity whatsoever. However, according to a Machian school of thought [28] and the *general principle of relativity* [29], all inertial effects observed in noninertial frames may be explained as due to the gravitational field of the "rest of the universe." In the present model, using the rest frame of the wall, one sees freely falling particles outside the bubble being accelerated inward, and indeed, from this point of view, the notion of positive gravitational mass makes sense globally.

The global space-time structure of the walls considered here exhibit nontrivial causal structures due to the presence of AdS_4 regions and their associated Cauchy horizons. Cauchy horizons imply that the coordinate extensions necessary for providing geodesically complete space-time manifolds are nonunique. Such ambiguities in the geodesic extensions are reminiscent of those in the Reissner-Nordström and Kerr black hole space-times [30,31]. These space-times form an infinite lattice [32,33]. The same lattice structure is possible in certain domain wall systems considered here, and it is even possible to formally associate the local parameters of the space-times in the following manner: the mass M and the charge Q (for the Reissner-Nordström black hole) or the angular momentum a (for the Kerr black hole) are associated with the energy density, σ, of the wall and the cosmological constant, $\Lambda \leq 0$, of the adjacent vacuum, respectively. The nontrivial causal structure in the domain wall system is obtained without the space-time singularities of the black holes. The absence of singularities opens the possibility of studying physics on causally nontrivial space-times, with asymptotically Minkowski regions in certain cases, without the problems presented by the

black hole curvature singularities.

The paper is organized as follows. In Sec. II, by working in the comoving frame of the wall, we deduce the local properties of space-time close to the wall and the topology of the wall itself. Then in Sec. III we find geodesic extensions of the comoving coordinate patch and discuss the global properties of the wall space-times. It is here that the similarities in the global structure of the nonextreme domain wall space-times to the global structure of black hole geometries are pointed out. Section IV contains a discussion of the results. Appendix A presents the local coordinate transformations between the comoving coordinates derived in the text and the conventional coordinates of the vacuum AdS_4, M_4, and de Sitter (dS_4) space-times. In Appendix B we review the salient aspects of AdS_4 useful for understanding the local and global properties of the walls discussed in this paper.

II. LOCAL PROPERTIES OF DOMAIN WALL SPACE-TIMES

In this section we present the local properties of the space-time induced by a class of vacuum domain walls in Einstein gravity. These walls are created from a scalar field source and separate vacuum space-times of zero, positive, and negative cosmological constants. We shall study explicitly only infinitely thin domain walls, and thus employ Israel's formalism [34,35] of singular hypersurfaces. This method is a familiar and well-defined approach to solving Einstein's equations in the limit where the matter source is approximated as an infinitely thin surface.

To begin with, we give general arguments in regard to the form of the space-time metric consistent with the symmetries of the domain wall background. Then we present Israel's formalism to determine the matching conditions of the space-time at the wall's world tube. We classify the solutions and discuss their effective gravitational fields using Tolman's [7] concept of gravitational mass.

A. Metric ansatz

We solve Einstein's gravitational field equations using certain symmetry constraints consistent with properties of a space-time induced by a domain wall source. In general, the solutions are time dependent. It is most convenient to describe the metric in the comoving coordinates of the wall system, i.e., in the rest frame of the wall. In this case, the stress energy associated with the wall is static and depends only on the coordinate z perpendicular to the wall.

First, we assume that the spatial part of the metric intrinsic to the wall and of the two-dimensional spatial sections "parallel" to the wall are *homogeneous* and *isotropic* in the *comoving frame* of the wall. Homogeneity and isotropy reduce the "parallel" metric to the spatial part of a (2+1)-dimensional Friedmann-Lemaître-Robertson-Walker (FLRW) metric [36]. In the conventional coordinates this metric has the form

$$(ds_{\parallel})^2 = R^2\left[(1-kr^2)^{-1}dr^2 + r^2 d\phi^2\right], \tag{2.1}$$

where R is independent of the coordinates r and ϕ. The scalar curvature of this surface is equal to $2k/R^2$.

There are three possible wall geometries. The first one is a planar wall with $k=0$. In this case the metric (2.1) can be transformed to Cartesian coordinates $(ds_{\parallel})^2 = R^2(dx^2+dy^2)$. The second possibility is a spherical wall with $k>0$. Then the wall is a closed bubble, in which case both r and ϕ are compact coordinates; i.e., one may introduce $r = k^{-1/2}\sin\theta$ which after a rescaling of R gives the line element $(ds_{\parallel})^2 = R^2(d\theta^2+\sin^2\theta d\phi^2)$. Finally, the wall could be a Gauss-Bólyai-Lobachevski surface with $k<0$. This negatively curved noncompact surface cannot be embedded in ordinary three-dimensional Euclidean space, that is, it cannot be pictured as an ordinary curved surface [37]. Writing $r = (-k)^{-1/2}\sinh\varrho$, with $\varrho>0$, and rescaling R brings the $k<0$ line element to $(ds_{\parallel})^2 = R^2(d\varrho^2+\sinh^2\varrho\, d\phi^2)$.

For our next assumption we demand that the two-dimensional space-time sections orthogonal to the wall are *static* as observed in the *rest frame* of the wall. Hence, if z denotes a coordinate describing the direction transverse to the wall and if t represents the *proper* time as measured by observers sitting on the wall, then $g_{tz}=0$, and both g_{tt} and g_{zz} depend only on z. By an appropriate choice of z coordinate we can write the orthogonal part of the metric as[1]

$$(ds_{\perp})^2 = A(z)\left(dt^2 - dz^2\right), \tag{2.2}$$

where $A(z)>0$. With $ds^2 \equiv (ds_{\perp})^2 - (ds_{\parallel})^2$ we get

$$ds^2 = A\left(dt^2-dz^2\right) - R^2\left[(1-kr^2)^{-1}dr^2 + r^2 d\phi^2\right], \tag{2.3}$$

where $A = A(z)$ and $R = R(t,z)$. The range of z is $z\in\langle-\infty,\infty\rangle$, and the range of the other coordinates is as in a FLRW cosmological model [36].

We shall now employ Einstein's equations to reduce the form of $R(t,z)$. With the metric (2.3) and the definition

$$H \equiv \frac{A'}{A}, \tag{2.4}$$

where $A' = \partial_z A(z)$, the nontrivial components of the Einstein tensor $G^{\mu}{}_{\nu} = \mathcal{R}^{\mu}{}_{\nu} - \frac{1}{2}\mathcal{R}^{\alpha}{}_{\alpha}g^{\mu}{}_{\nu}$ are

$$\begin{aligned}
G^t{}_t &= \tfrac{k}{R^2} - \tfrac{2R''}{AR} - \tfrac{R'^2}{AR^2} + \tfrac{HR'}{AR} + \tfrac{\dot R^2}{AR^2},\\
G^z{}_t &= \tfrac{2\dot R'}{AR} - \tfrac{H\dot R}{AR},\\
G^z{}_z &= \tfrac{k}{R^2} - \tfrac{R'^2}{AR^2} - \tfrac{HR'}{AR} + \tfrac{2\ddot R}{AR} + \tfrac{\dot R^2}{AR^2},\\
G^r{}_r &= G^{\phi}{}_{\phi} = -\tfrac{R''}{AR} + \tfrac{\ddot R}{AR} - \tfrac{H'}{2A},
\end{aligned} \tag{2.5}$$

[1] Throughout the paper we use geometric units of time, i.e., $c\equiv 1$.

where $\dot{R} = \partial_t R(t)$.

Since we are considering matter configurations which are static in the (t, z) plane, there is no energy flow in the z direction in the comoving frame of this coordinate system. Therefore, the $T^z{}_t$ component of the energy-momentum tensor vanishes. Then the (z, t) component of Einstein's field equations[2]

$$G^\mu{}_\nu = \kappa T^\mu{}_\nu, \tag{2.6}$$

imply $G^z_t = 0$ or

$$2\dot{R}' = H\dot{R}. \tag{2.7}$$

There are two possible solutions to Eq. (2.7). In the first case, when the metric is static, $\dot{R} = 0$, and Eq. (2.7) is trivially satisfied. Let us first focus on the other case when the metric is nonstatic. If R is time dependent, integration with respect to time yields

$$2R' = HR + M(z), \tag{2.8}$$

where $M(z)$ is an arbitrary function of z. A static matter source is defined by a static stress-energy tensor $T^\mu{}_\nu$, which, through Einstein's equations, implies a static Einstein tensor. A static G^r_r implies

$$\frac{\ddot{R}}{R} = \frac{R''}{R} + g(z), \tag{2.9}$$

where $g(z)$ is an arbitrary function of z. From the requirement of time independence of $G^t_t - G^z_z$ one finds that

$$\frac{2}{A}\left[-\frac{R''}{R} + \frac{HR'}{R} - \frac{\ddot{R}}{R}\right] = \frac{2}{A}\left[f(z) - g(z)\right], \tag{2.10}$$

where $f(z)$ is another arbitrary function of z. Using Eq. (2.9) and multiplying Eq. (2.10) by $\frac{1}{2}RA$ we get

$$-2R'' + HR' = f(z)R. \tag{2.11}$$

Adding the z derivative of Eq. (2.8) one finds

$$M'(z) = [H' + f(z)]R. \tag{2.12}$$

This equation holds for any t only if $M'(z) = 0$ and $f(z) = -H'$. Hence, $2R' = HR + M_0$ where M_0 is a constant.

A thick wall solution can be pictured as a stack of infinitely thin walls. If we require that each of the thin walls are boost invariant along surfaces of constant z, i.e., each surface of constant z has an *exterior curvature* which is boost invariant, it follows that $M_0 = 0$. In the static case ($\dot{R} = 0$), the same symmetry constraint implies $R^2 \propto A$. In general, this symmetry is stronger than just requiring a boost-invariant $T^\mu{}_\nu$ because it involves only first-order derivatives of the metric coefficients (see Sec. II B 1 below), whereas $T^t_t = T^r_r$ involves a second-order differential equation. Also in the thin wall case, the gravitational field on either side could have a Kasner-type behavior compensating each other in such a way that the interpolating singular surface still is boost invariant [38]. We shall, however, assume that the gravitational field inherits the symmetry of the source, and that the directions parallel to the wall are boost invariant in the strong sense. The line element we shall examine is thus given by

$$ds^2 = A(z)\{dt^2 - dz^2 - S^2(t)[(1 - kr^2)^{-1}dr^2 + r^2 d\phi^2]\}. \tag{2.13}$$

In summary, the assumptions which imply the form of the metric (2.13) are the following:

1. The spatial part of the metric intrinsic to the wall is *homogeneous* and *isotropic.*
2. The space-time section orthogonal to the wall is *static.*
3. The directions parallel to the wall are *boost invariant* in the strong sense.[3]

To solve the Einstein equations for the two metric functions $A(z)$ and $S(t)$, we follow the approach of Israel [34] which approximates the wall as infinitely thin in the z direction. Thick walls will have the same $S(t)$ as found in the thin wall approximation and will asymptotically[4] approach the thin wall result for $A(z)$. For detailed discussions of this formalism, with emphasis on domain walls, see Refs. [9,39–41] and Ref. [42] for an application to a static plane-symmetric geometry.

B. Thin wall approximation

We assume that the properties of the gravitational field outside a domain wall can be deduced without knowledge of the internal structure of the wall. For this reason we employ the thin wall approximation. In this approximation, the wall is treated as infinitely thin, and consequently its energy-momentum tensor has a δ-function singularity at the wall. Einstein's field equations imply that the Einstein tensor also must have a δ-function singularity here. Because Einstein's tensor is of second order in derivatives of the metric, such a singular hypersurface may be modeled by a metric tensor which has a discontinuity in its first-order derivatives in the direction transverse to the singular surface. This idea is the basis of Israel's formalism [34] for singular layers in general relativity. Furthermore, we shall assume that the wall is a *domain wall,* that is, the wall itself has a vacuumlike surface energy-momentum tensor. By this we mean a sur-

[2]The Einstein constant κ is defined by $\kappa \equiv 8\pi G$, where G is Newton's constant.

[3]As shown in Sec. II B 2, boost invariance also puts restrictions on the functional form of the time dependence, $S(t)$.

[4]For the familiar kink matter sources, which we are considering, the solutions typically approach the thin wall results exponentially fast over its characteristic length scale.

face energy-momentum tensor which is proportional to the metric intrinsic to the world tube of the wall. Physically, one notes that there is no way to measure velocity relative to a vacuum and thus a vacuum must have a boost invariant energy-momentum tensor. This leads to the specific form of the surface energy-momentum tensor.

1. Israel's matching conditions

Consider a thin wall placed at a *constant* z-coordinate position in a space-time described by the metric (2.13). According to Israel's formalism [34], the surface energy-momentum tensor of the wall is described by the Lanczos tensor, $\mathcal{S}^i_{\ j}$, which is given by

$$\kappa\mathcal{S}^i_{\ j} = -[K^i_{\ j}]^- + \delta^i_{\ j}[K]^-, \tag{2.14}$$

where $K^i_{\ j}$ is the extrinsic curvature. The square brackets $[\ \ ]^-$ signify the discontinuity at the wall placed at $z = z_0$, i.e., $[\Omega]^- \equiv \Omega_2 - \Omega_1$, where Ω_2 and Ω_1 are the $\epsilon \to 0$ limit of $\Omega(z_0 + \epsilon)$ and $\Omega(z_0 - \epsilon)$, respectively. The coordinates $x^i \in \{t, r, \phi\}$ describes the space-time parallel to the wall. The extrinsic curvature is given by the covariant derivative of the spacelike unit normal n^μ of the wall's hyper-space-time:

$$K^i_{\ j} \equiv -n^i_{\ ;j}\,, \tag{2.15}$$

where n^μ is specified by the defining relations

$$n^\mu n_\mu \equiv -1 \quad \text{and} \quad n^\mu u_\mu \equiv 0. \tag{2.16}$$

Here u^μ is the four velocity of an observer following the wall. In the present case, $u^\mu = \delta^\mu_{\ t}$ when represented in the coordinate system of the metric (2.13). Since the wall is at a *constant* z coordinate, the extrinsic curvature takes a simple form if we use a coordinate system in which the spatial coordinate transverse to the wall, $\hat{z}$, is normalized so that $g_{\hat{z}\hat{z}} = -1$, i.e., $d\hat{z} = A^{1/2}dz$. In these coordinates

$$K_{ij} = -\frac{\zeta}{2}g_{ij,\hat{z}}\,, \tag{2.17}$$

where $\zeta = \pm 1$ is a sign factor coming from the inherent sign ambiguity of the unit normal n^μ. ζ will be determined by insisting that the wall corresponds to the thin limit of a kinklike source.

We choose to scale the coordinates such that $A(z_0) = 1$ where z_0 is the position of the wall. Then, without loss of generality we may perform a global translation of the z coordinate so as to bring the origin of the z axis to the position of the wall. In this way we find

$$\kappa\mathcal{S}^i_{\ j} = -\delta^i_{\ j}[\zeta H]^-_{z=0} \tag{2.18}$$

corresponding to a vacuumlike equation of state. In other words, the surface energy density σ given by

$$\kappa\sigma \equiv \kappa\mathcal{S}^t_{\ t} = -[\zeta H]^-_{z=0}, \tag{2.19}$$

is equal to the wall's tension, $\tau \equiv \mathcal{S}^r_{\ r} = \mathcal{S}^\phi_{\ \phi}$.

2. Vacuum solutions

To describe the gravitational field exterior to the wall, we need the solution to Einstein's field equations. Here we consider thin domain walls interpolating between two maximally symmetric vacua of zero, positive, or negative cosmological constant. Maximally symmetric vacuum solutions to Einstein's theory are well known [36]; nevertheless, we rederive them below using the comoving coordinate system of the wall configurations. The reason to employ the comoving frame is twofold: the first one is technical; Israel's matching conditions across the wall region are easily satisfied in this frame. The second reason is that in this frame the space-time exhibits cosmological horizons with properties closely related to the ones of the corresponding black holes. In Appendix A we present the local coordinate relations between the metric in the rest frame of the wall and the more conventional coordinates of maximally symmetric space-times.

Using the metric (2.13) and the definition (2.4), the Einstein tensor takes the form

$$\begin{aligned} G^t_{\ t} &= \tfrac{1}{A}\left(\tfrac{k}{S^2} - H' - \tfrac{1}{4}H^2 + \tfrac{\dot{S}^2}{S^2}\right), \\ G^z_{\ z} &= \tfrac{1}{A}\left(\tfrac{k}{S^2} - \tfrac{3}{4}H^2 + \tfrac{2\ddot{S}}{S} + \tfrac{\dot{S}^2}{S^2}\right), \\ G^r_{\ r} &= G^\phi_{\ \phi} = \tfrac{1}{A}\left(-\tfrac{1}{4}H^2 - H' + \tfrac{\ddot{S}}{S}\right). \end{aligned} \tag{2.20}$$

With a static $T^\mu_{\ \nu}$, and hence static $G^\mu_{\ \nu}$, one finds $\ddot{S}/S = q_0$ where q_0 is a real constant. Then because of boost invariance in the r and ϕ directions, $G^t_{\ t} = G^r_{\ r}$, and consequently

$$\frac{\ddot{S}}{S} = q_0 = \frac{\dot{S}^2}{S^2} + \frac{k}{S^2}. \tag{2.21}$$

With this result, $G^z_{\ z} = \Lambda$ implies

$$\frac{1}{4}H^2 = q_0 - \frac{\Lambda}{3}A, \tag{2.22}$$

where consistency demands $\Lambda A(z) \le 3q_0$. Note that we shall sometimes parametrize the cosmological constant by $\Lambda = \pm 3\alpha^2$. Equations (2.21) and (2.22) are the fundamental equations yielding the line elements which we study. Note that the $A = 1$ solution of Eq. (2.22) is a valid solution of the other components of the Einstein equations only for the case $q_0 = \Lambda = 0$.

The geometry of hypersurfaces of constant z is determined by solutions to Eq. (2.21). Without loss of generality we normalize the curvature constant to $k \in \{-\beta^2, 0, \beta^2\}$. The solutions of Eq. (2.21) are classified according to the sign of q_0. Thus up to a global translation of the time coordinate,

$$S_- = \sin\beta t, \qquad k = -\beta^2, \tag{2.23}$$

$$S_0 = \begin{cases} \beta t, & k = -\beta^2, \\ 1, & k = 0, \end{cases} \tag{2.24}$$

$$S_+ = \begin{cases} \sinh\beta t, & k = -\beta^2, \\ e^{\beta t}, & k = 0, \\ \cosh\beta t, & k = \beta^2, \end{cases} \tag{2.25}$$

where the subscripts on S refer to the sign of q_0. With these solutions for $S(t)$, the sections of constant z are (2+1)-dimensional spaces of maximal symmetry, i.e., these hyperspaces are AdS_3, M_3, and dS_3 space-times, respectively. Note that the line element (2.13) is quadratic in $S(t)$. Hence, the overall sign of S is arbitrary. In addition, since a change in the sign of β is equivalent to time reversal in all the solutions for $S(t)$, choosing $\beta \geq 0$ implies no loss of generality.

The solutions for $A(z)$ from Eqs. (2.4) and (2.22) are the following:

$$A_- = \beta^2[\alpha\cos(\beta z + \vartheta)]^{-2}, \qquad \Lambda = -3\alpha^2 \leq -3\beta^2, \tag{2.26}$$

$$A_0 = \begin{cases} (\alpha z - 1)^{-2}, & \Lambda = -3\alpha^2, \\ 1, & \Lambda = 0, \end{cases} \tag{2.27}$$

$$A_+ = \begin{cases} \beta^2[\alpha\sinh(\beta z - \beta z')]^{-2}, & \Lambda = -3\alpha^2, \\ e^{\pm 2\beta z}, & \Lambda = 0, \\ \beta^2[\alpha\cosh(\beta z - \beta z'')]^{-2}, & \Lambda = 3\alpha^2 \leq 3\beta^2, \end{cases} \tag{2.28}$$

where the subscripts on A refer to the sign of q_0. Without loss of generality we have moved the origin of the z axis to the position of the wall ($z_0 = 0$). The three integration constants ϑ, z', and z'' are determined by the requirement that $A(0) = 1$. This normalization yields

$$\vartheta_\pm = \pm\arccos(\beta/\alpha), \tag{2.29}$$

$$\beta z'_\pm = \frac{1}{2}\ln\left[1 + \frac{2\beta^2}{\alpha^2} \pm \frac{2\beta}{\alpha^2}(\alpha^2 + \beta^2)^{1/2}\right], \tag{2.30}$$

$$\beta z''_\pm = \frac{1}{2}\ln\left[-1 + \frac{2\beta^2}{\alpha^2} \mp \frac{2\beta}{\alpha^2}(\beta^2 - \alpha^2)^{1/2}\right]. \tag{2.31}$$

The constants $\beta z'$ and $\beta z''$ satisfy $e^{2\beta(z'_+ + z'_-)} = e^{2\beta(z''_+ + z''_-)} = 1$ and $e^{2\beta z''_-} > 1 > e^{2\beta z''_+}$ and $e^{2\beta z'_-} \leq 1 \leq e^{2\beta z'_+}$ where in the last case, equality is obtained when $\beta = 0$. As one can see from Eq. (2.31), there is no extreme limit ($\beta \to 0$) in the de Sitter case.

Recall that the solutions (2.26)–(2.28) are the form for the metric function $A(z)$ some distance away from a wall centered at $z = 0$. In the A_- solution (2.26), z is an angular coordinate, but as seen from Eq. (2.23), the metric has singularities for certain values of comoving time t and because of this, this solution will not be further discussed here.

Points where $A(z)$ is singular represent affine boundaries of the space-time. They are an infinite proper distance away from every other point within the particular interval of z considered. The first of the A_0 solutions (2.27) is the line element for AdS_4 written in the so-called *horospherical* coordinate system. Discussions of these coordinates can be found in Refs. [17,19,20]. For the first two $q_0 = \beta^2$ solutions, one is able to consider both singular or nonsingular functions $A(z)$ depending on the choice of $\pm\beta$ or $\beta z'_\pm$ for the respective solutions $\Lambda = 0$ or $\Lambda = -3\alpha^2$. For example, if we choose $A = e^{+2\beta z}$ for $z > 0$ (the M_4 side of a wall), there will be a coordinate singularity at $z = \infty$ corresponding to the null boundary of the space-time. Choosing the decaying exponential will cause $z = \infty$ to be a finite proper distance away from any other point; thus the coordinate patch must be extended. Likewise, choosing $\beta z'_-$ for $z < 0$ (the AdS_4 side) will result in a timelike coordinate singularity at $z = z^*$, where $z^* = z'_-$. This coordinate singularity is again the boundary of the space-time, only now it is timelike rather than null as in the M_4 case. The de Sitter solution is always without coordinate singularities. Geodesic extensions of the domain wall space-times will be further discussed in Sec. III.

3. *Topology of the walls*

On account of boost invariance in the directions parallel to the wall, the spatial curvature of constant-z sections is not unambiguously defined. Since the wall is homogeneous and boost invariant, there is no preferred frame in the (2+1)-dimensional space-time of the wall. Observers can measure the curvature of space by sending light signals to each other and measuring angles of triangles, but the results will depend on the relative motion of these observers. For instance, the two S_0 solutions (2.24)—the Milne-type solution with $S = \beta t$ and $k = -\beta^2$ and the inertial Minkowski solution with $S = 1$ and $k = 0$—are related by a coordinate transformation [43] not involving the transverse coordinate z and therefore describe locally equivalent space-times.[5] Similarly, the constant-z sections of the three S_+ solutions (2.25) all represent (2+1)-dimensional de Sitter space-time (dS_3). The topology of dS_3 is $\mathbf{R}$(time) $\times$ $\mathbf{S}^2$(space). Embedded in a flat higher-dimensional Minkowski space-time, dS_3 represents a hyperboloid [19], and the three possible spatial curvatures correspond to three different choices of constant time slices of this hyperboloid [30,43]. Just as in the four-dimensional case [30,43], only the positive curvature solution gives a complete covering of dS_3.

[5]The same holds in (3+1) dimensions where a special set of observers see flat Minkowski space-time as the expanding Milne universe [43] with hyperbolic spatial sections.

Therefore, of the three S_+ solutions in Eq. (2.25), only the one corresponding to a compact *spherical wall* with radius $\beta^{-1}A(z)^{-1/2}S(t)$ completely covers the constant-z space-time. The S_0 solution is the *only* wall which represents a noncompact *planar* ($k = 0$) wall. In summary, homogeneity, isotropy, and geodesic completeness of the space-time intrinsic to the wall as described in comoving coordinates impose constraints on the topology of the domain wall; it either corresponds to a *static, planar* wall or to a *time dependent bubble*:

$$S_0 = 1 \text{ and } k = 0 \quad or \quad S_+ = \cosh\beta t \text{ and } k > 0. \tag{2.32}$$

Note again that the solutions $S(t)$ are valid in the thick wall case because its functional form is determined by the requirement of boost invariance alone and thus independent of $A(z)$. The solutions for $A(z)$ in Eqs. (2.27) and (2.28) approximate the local form of the metric some distance away from the wall. To describe the space-time on both sides of the wall centered at $z = 0$, we fix the same value for the parameter q_0 and the curvature k on both sides and choose any of the corresponding solutions for $A(z)$. Consequently, there are two distinct wall configurations described by the line element (2.13): one whose spatial topology parallel to the wall surface is $\mathbf{R}^2$ and another whose topology is $\mathbf{S}^2$.

We would like to elaborate on the closed bubble solution [$k = \beta^2$, $S(t) = \cosh\beta t$]. First, we transform to canonical $\mathbf{S}^2$ coordinates in Eq. (2.13). Writing $\beta r = \sin\theta$, brings the metric to

$$ds^2 = A(z)\left[dt^2 - dz^2 - \beta^{-2}\cosh^2\beta t\,(d\theta^2 + \sin^2\theta d\phi^2)\right]. \tag{2.33}$$

For these solutions, *both* sides of the wall have a compact spherical line element in the spatial directions parallel to the wall. Thus, observers on *each* side of the wall observe the bubble wall collapsing from an infinite radius at $t = -\infty$ to a finite radius at $t = 0$ and then reexpanding to an infinite radius at $t = \infty$.

This may sound strange since the wall is located at a fixed z coordinate. However, the proper surface area of the bubble is given by $4\pi R_b^2 \equiv 4\pi\beta^{-2}A(z)S^2(t)$, which means that the radius as measured by this formula is time dependent. Geometrically, R_b is the *radius of curvature* of the wall; physically, it is a measure of the proper size of the bubble. Hence, the bounce description is not a coordinate artifact. Indeed, observers sitting on the bubble and measuring its surface area with *standard* measuring rods extending around the bubble, versus time as measured by *standard* clocks, will observe the bounce directly.

Notice also that for the bubble solution, the direction orthogonal to the wall is described by the z coordinate, which has the range $\langle -\infty, \infty\rangle$. This is twice the range of a radial coordinate in Euclidean space. However, it is R_b rather than z which plays the role of the radius. Moreover, when looking at the z dependence of R_b at constant t, R_b can either decrease on both sides of the bubble or increase on one side and decrease on the other. In the former case, using measurements of angular distance, observers on both sides of the wall can rightfully say that they are on the *inside* of the bubble. In this picture $z \in \langle -\infty, 0]$ and $z \in [0, \infty\rangle$ map onto twice $R_b \in [0, R_0]$, where $R_0 = \beta^{-1}S(t)A^{1/2}(0)$, i.e., the infinite range of z maps onto two ranges for the angular distance corresponding to two spheres (the two insides of the bubble). In the latter case, $z \in \langle -\infty, 0]$ and $z \in [0, \infty\rangle$ map onto $R_b \in [0, R_0]$ and $R_b \in [R_0, \infty\rangle$, corresponding to the *inside* and the *outside* of a single bubble. As we shall see later on, there is no physical bubble solution (no solution with surface energy $\sigma > 0$) corresponding to a space where both observers are on the outside of the bubble. We conclude that a spherical vacuum domain wall has at least *one* inside.

For the $q_0 = 0$ and $q_0 = \beta^2$ wall solutions, the constant z sections correspond to M_3 and dS_3, respectively. The novel causal structure for the walls, which we shall discuss in Sec. III, involves only the (1+1)-dimensional sections orthogonal to the walls. This structure is deduced from an analysis of the (t, z) components of the line elements.

4. Surface energy density of the domain walls

By matching vacuum solutions with the same k and q_0 and using Eqs. (2.19) and (2.22), we find that the interpolating domain walls have the following surface energy density, σ, and tension, $\tau = \sigma$:

$$\kappa\sigma = 2\zeta_1 h_1\left(q_0 - \frac{\Lambda_1}{3}\right)^{1/2} - 2\zeta_2 h_2\left(q_0 - \frac{\Lambda_2}{3}\right)^{1/2}, \tag{2.34}$$

where the indices 1 and 2 stand for values at $z < 0$ and $z > 0$, respectively.

In the thin wall formalism, there is an ambiguity in the sign of the unit normal n^μ defined in Eq. (2.16). Also in going from Eq. (2.22) to Eq. (2.34), we pick up another sign ambiguity because Eq. (2.22) is quadratic in H. These sign ambiguities are taken care of by the sign factors $h_i = \pm 1$ and $\zeta_i = \pm 1$ with $i \in \{1, 2\}$. The first sign factor h_i is determined as follows. If A_i is an increasing function of z, then $h_i = 1$, and conversely if A_i is decreasing then $h_i = -1$. Physically relevant solutions to the matching conditions involve those with a *positive* energy density σ as well as sources corresponding to the infinitely thin wall limit of a kinklike source. Associating the direction of the wall's outward normal with a chosen direction of the matter source gradient implies $\zeta_1 = \zeta_2 = 1$ for a kink-type source. Sources with $\zeta_1 = -\zeta_2$ correspond to spike-type sources which we do not consider. We will choose to orient the z coordinate so that the vacuum of lowest energy (most negative Λ) will be placed on the $z < 0$ side.

C. Classification of the domain wall solutions

The previous solutions can be classified according to the three values of the parameter q_0. The metrics written

here in the comoving frame are locally related to more standard coordinates of M_4, AdS_4, and dS_4, depending on the cosmological constant $\Lambda = 0, \Lambda < 0$, or $\Lambda > 0$, respectively. We exhibit these relations in Appendix A.

In the case $q_0 = -\beta^2$, the line element intrinsic to the wall has periodic singularities in comoving time. Therefore, we do not consider it further here. The possibilities $q_0 = 0$ and β^2 are classified in the following two subsections.

1. Extreme walls ($q_0 = 0$)

The $q_0 = 0$ solutions exist for AdS_4 ($\Lambda = -3\alpha^2$) and for M_4 ($\Lambda = 0$), the latter being the $\Lambda \to 0$ limit of the former. If the vacua between which the domain wall interpolates are supersymmetric, then these walls are realized as supersymmetric bosonic configurations in $N = 1$ supergravity coupled to chiral matter superfields [15]. In this case, the walls are called *extreme* domain walls [18] in analogy with the extreme Reissner-Nordström black hole, which is also realized as a supersymmetric bosonic configuration [44].

The line element (2.13) for the $q_0 = 0$ case has two physically distinct solutions: $S = 1$ and the two solutions for $A(z)$ of Eq. (2.27). The solutions are written in canonical M_4 Cartesian coordinates and *horospherical* AdS_4 coordinates, respectively. The horospherical coordinates are natural for describing AdS_4 when it is juxtaposed with a flat M_4 region, as it is in the $k = 0$ extreme wall [18–20].

The extreme walls [23] have been classified into three types according to the nature of their space-times [17]. Type I is the planar wall interpolating between M_4 and AdS_4. Type II walls interpolate between two AdS_4 regions with the metric conformal factor $A(z)$ becoming $(\alpha_i z)^{-2}$ on the respective sides ($i \in \{1, 2\}$) of the wall. Type III walls interpolate between two AdS_4 spaces with different cosmological constants in such a way that the conformal factor increases without bound for z moving away from the wall on one side. The singularity in $A(z)$ represents the timelike boundary of the space-time, i.e., affine infinity. In the underlying supergravity theory, Type I, II, and III walls can also be distinguished by the behavior of the superpotential as the wall interpolates between the two supersymmetric vacua [17].

The energy density of the extreme walls is

$$\kappa\sigma_{\text{ext}} = 2(\alpha_1 \pm \alpha_2), \tag{2.35}$$

where $\Lambda_i = -3\alpha_i^2$ with the plus sign for Type II walls and the minus sign for Type III walls. It is understood that $\alpha_1 > \alpha_2$ in the latter case. Type I corresponds to $\alpha_2 = 0$. By using the thin wall approximation, a reflection symmetric special case of Type II walls was independently found by Linet [14].

2. Non- and ultraextreme walls ($q_0 = \beta^2$)

The $q_0 = \beta^2$ solutions exist for closed walls for all values of the cosmological constant. Specifically, we have the four physically distinct solutions (2.28) for $A(z)$.

A nonextreme wall has an energy density higher than the corresponding extreme wall. Explicitly, the energy density is

$$\kappa\sigma_{\text{non}} = 2\left(\pm\alpha_1^2 + \beta^2\right)^{1/2} + 2\left(\pm\alpha_2^2 + \beta^2\right)^{1/2}. \tag{2.36}$$

Here $\Lambda_i = \mp 3\alpha_i^2$, so that a minus sign in front of α^2 in the above expression corresponds to a *positive* Λ term. In the de Sitter case $\alpha_i^2 \leq \beta^2$ [39].

The "planar" reflection symmetric wall discussed by Vilenkin [45] and Ipser and Sikivie [9] with $\Lambda_1 = \Lambda_2 = 0$ is a special nonextreme wall. These walls have an energy density $\kappa\sigma = 4\beta$. Thick wall generalizations have been studied in Refs. [46,47]. Note that these walls are spherically symmetric bubbles [19] rather than planar walls. For all the nonextreme walls, the radius of curvature R_b of concentric shells at constant time *decreases* away from the bubble on *both* sides. Hence, in this sense, the nonextreme bubbles have *two* insides.

An ultraextreme wall has an energy density lower than the corresponding extreme wall. Its energy density is

$$\kappa\sigma_{\text{ultra}} = 2\left(\pm\alpha_1^2 + \beta^2\right)^{1/2} - 2\left(\pm\alpha_2^2 + \beta^2\right)^{1/2}. \tag{2.37}$$

The signs in front of α^2 correspond to $\Lambda_i = \mp 3\alpha_i^2$. It follows that if $\Lambda_i = 3\alpha_i^2$, then $\alpha_i^2 \leq \beta^2$ [39].

Ultraextreme AdS_4–AdS_4 and AdS_4–M_4 bubbles of the false vacuum decay are more like ordinary bubbles than nonextreme bubbles; their radii increase away from the wall on one side and decrease on the other. Thus, they have one inside and one outside, the outside being the higher energy vacuum. M_4–dS_4 and dS_4–dS_4 walls were addressed in Refs. [39–41].

In the static or extreme limit $\beta \to 0$, the nonextreme and ultraextreme walls of AdS_4–AdS_4 walls reduce to Type II and Type III extreme walls, respectively. The non- and ultraextreme bubbles were discussed by Berezin, Kuzmin, and Tkachev [24] with particular emphasis on the ultraextreme bubbles corresponding to false vacuum decay.

D. Fiducial observers and Tolman's mass for extreme walls of Type I and Type II

1. Fiducial observers

Inertial observers on the M_4 side of the extreme AdS_4–M_4 wall experiences no gravitational effects[6] from the infinite wall. A particular way to understand this result is to investigate the proper acceleration,[7] $a^{\hat{\mu}}$, necessary to be a fiducial observer (an observer at a fixed spatial

[6]Strictly speaking the "gravitational force" is exponentially close to zero (exactly zero in the thin wall approximation), which is consistent with the appellation "Minkowski side."

[7]Hats denote tensor components relative to a (pseudo)-orthonormal tetrad frame, i.e., a physical frame.

position) in the space-time described by the conformally flat metric $A(z)(dt^2-dx^2-dy^2-dz^2)$. This acceleration is given by [17]

$$a^{\hat{\mu}} = \tfrac{1}{2}A^{-1/2}H\delta^{\hat{\mu}}{}_{\hat{z}} \tag{2.38}$$

and is directed *toward* the wall region thus exhibiting "repulsive gravity." Clearly for $A(z)=1$ the acceleration is zero, and no gravitational effects are felt.

On the AdS_4 side, $A(z)=(\alpha z-1)^{-2}$, which yields a constant proper acceleration of magnitude α for fiducial observers. Observe that this acceleration is *half* the surface mass density of an AdS_4–M_4 wall. This fact will prove important in the following formulation of the Tolman mass per area for the domain wall system.

2. *Tolman's mass per area*

A useful way to understand the equilibrium between the extremal wall and the adjacent space-times is to compute Tolman's effective gravitational mass for the system. In spaces of high symmetry it is possible to rewrite Einstein's field equations as an integral which can be interpreted as an expression for an effective gravitational mass. By computing this mass one can understand the effective "gravitational forces" and their sources.

For example, in pure AdS_4, the effective gravitational mass per volume is positive, thus indicating the attractive nature of the gravitational field produced by the negative energy vacuum. As discussed in Appendix B, the motion of test particles is oscillatory in pure AdS_4 reflecting the fact that every point in the space-time attracts the particles with its positive effective mass density. The converse holds for pure dS_4, which is a familiar result from inflationary cosmology where the repulsive nature of a positive energy vacuum drives the universe into exponential expansion.

In the domain wall system, the relevant object is the gravitational mass per area. In particular, the zero Tolman's mass of the extreme AdS_4–M_4 domain wall enables one to understand why it is possible to be on the M_4 side and near the infinite wall, which possesses a nonzero mass density, and yet feel no gravitational effects.

Tolman's formula for the gravitational mass was originally derived for a static spherically symmetric metric [7]. We generalize this result to the case of the static planar symmetry of Types I and II extremal walls. In the derivation of Tolman's mass formula one focuses on the *generalized surface gravity,*[8] that is, the gravitational acceleration as measured with *standard* rods and *coordinate* clocks [49]

$$k^i \equiv -\sqrt{g_{tt}}a^{\hat{i}}. \tag{2.39}$$

Since we are seeking a "Newtonian" concept of gravitational mass, it is natural to use *coordinate* time instead of the local proper time because the latter time is subject to time-dilation effects, which we eliminate by the factor of $\sqrt{g_{tt}}$. Note that only in the case where this coordinate time becomes the proper time of the observers (e.g., at infinity) is one guaranteed a direct physical interpretation of this mass. In the Schwarzschild case, for instance, the Tolman mass obtained by integrating from the origin to the surface of a finite, static source, is identical to the M parameter in the Schwarzschild metric describing the vacuum exterior to the source. For a metric as given in Eq. (2.13), with $S(t)=1$, the generalized surface gravity is

$$k^i = -\tfrac{1}{2}H\delta^i{}_z\,. \tag{2.40}$$

In a spherically symmetric four-dimensional space-time, one relates k^r to the Tolman mass by defining a mass M in such a way that the Newtonian force law is reproduced: $GM \equiv -r^2k^r$, and in the three-dimensional case $G_3M_3 \equiv -rk^r$, where G_3 is the (2+1)-dimensional Newton's constant [50]. In the plane-symmetric four-dimensional case, considered here, we deal with an essentially two-dimensional problem, and the appropriate Newtonian force law implies $\kappa\Sigma \equiv -2k^z$ where Σ is the gravitational mass per area of the plane. The factor of 2 is included because the gravitational acceleration is half the mass per area in the planar symmetric case (in the reflection symmetric case [45,51] one finds that the acceleration on both sides is a quarter of the mass density). In the same spirit as the compact spherically symmetric case, Eq. (2.40) leads to

$$\kappa\Sigma(z) = H(z). \tag{2.41}$$

For this equation to make sense in the wall case we rewrite the right-hand side in terms of an integral. Starting from the Einstein tensor (2.20) one finds (in the static case $q_0=0$)

$$G^t{}_t - G^z{}_z - G^r{}_r - G^\phi{}_\phi = \frac{A''}{A^2}. \tag{2.42}$$

Using $\sqrt{-g^{(4)}}=A^2$, $\sqrt{g^{(2)}}=A$, $G^\mu{}_\nu = \kappa T^\mu{}_\nu$, and Eq. (2.42), we can rewrite the right-hand side of Eq. (2.41) as the following integral expression:

$$\kappa\Sigma(z) = H(z) = \frac{\kappa\int_{-\infty}^{z}\sqrt{-g^{(4)}}dz'\left(T^t{}_t - T^z{}_z - T^r{}_r - T^\theta{}_\theta\right)\int dxdy}{\sqrt{g^{(2)}(z)}\int dxdy}, \tag{2.43}$$

where we used $A'(-\infty)=0$, as is the case for both the asymptotically M_4 and AdS_4 sides of Types I and II extremal walls. The numerator on the right-hand side of Eq. (2.43) is recognized as the Tolman mass of a static space-time [7]. This mass is nonlocal, which is consistent

[8] In black hole theory [48] the term *"surface gravity"* means the acceleration at the horizon surface. By the *"generalized surface gravity"* we mean the acceleration of gravity at any surface.

with it giving a Newtonian perspective to a static space-time. Basically, the Tolman mass formula expresses the fact that mass and energy are equivalent quantities in relativistic physics. On account of this, energy in the form of pressure contributes to the gravitational field along with the mass density. In this vein, one can define a gravitational mass density by $\rho_g \equiv \rho + 3p$ for a perfect fluid in $3+1$ dimensions. In the limit where we integrate from $z = -\infty$ to $z = \infty$, we get $\Sigma(\infty) = 0$. This means that the total gravitational mass of Types I and II extreme space-times is zero. It should be noted that Type III space-time is causally identical to pure AdS_4 (see Sec. III). Therefore, the effective mass per volume of this system is the relevant object; the effective mass per area, as with pure AdS_4, is infinite.

3. Tolman's mass per area of a thin extreme wall

In the thin-wall approximation we can distinguish contributions to the Tolman mass per area due to the wall itself and due to the vacuum energy of the adjacent space-time. In this case, a domain wall has an effective gravitational mass per area, $\Sigma_{\rm wall} = S^t{}_t - S^r{}_r - S^\phi{}_\phi$, given by $\Sigma_{\rm wall} \equiv \sigma - 2\tau$. Since the tension τ is equal to the energy density σ for a vacuum domain wall [see Eqs. (2.18) and (2.19)], we find $\Sigma_{\rm wall} = -\sigma < 0$. By use of Eq. (2.35) one finds that $\kappa\sigma = 2\alpha$, which yields

$$\kappa\Sigma_{\rm wall} = -2\alpha. \tag{2.44}$$

This negative gravitational mass per area for the wall, with its *repulsive* gravity, must be compensated by a positive gravitational surface mass density from the AdS_4 space-time on the AdS_4 side of the wall in order for there to be no force on the M_4 side. This is precisely the case as we now show. Again, taking into account the effect of vacuum pressure, $p_v = -\rho_v$, the gravitational mass density of AdS_4 is

$$\kappa\rho_g = \Lambda - 3\Lambda = 6\alpha^2. \tag{2.45}$$

Integrating out the z direction from $z = -\infty$ to the position of the wall at $z = 0$ yields the following mass per area for the AdS_4 side of the wall:

$$\kappa\Sigma_{\rm AdS} = \lim_{z\to 0}\left[\frac{\int_{-\infty}^{z}(6\alpha^2)\sqrt{-g^{(4)}}dz\int dxdy}{\int\sqrt{g^{(2)}}dxdy}\right]$$

$$= \lim_{z\to 0}\left[-\frac{2\alpha}{(\alpha z - 1)}\right] = 2\alpha. \tag{2.46}$$

Hence, as seen from the M_4 side of the domain wall (the $z > 0$ side), there are two gravitational surface mass densities on the $z \le 0$ side. First, there is a *negative* mass per area coming from the domain wall: $\kappa\Sigma_{\rm wall} = -2\alpha$. Second, there is a *positive* integrated mass per area coming from AdS_4 space itself: $\kappa\Sigma_{\rm AdS} = 2\alpha$, which exactly cancels that of the domain wall.

The analysis used for the extreme AdS_4–M_4 wall can also be applied to the extreme type II AdS_4–AdS_4 wall. When one side is M_4, the Killing time, t, corresponds to the proper time of an observer infinitely far away from the wall on the Minkowski side. In the Type II case, one may use an observer sitting in the center of the wall. Here too, there is a frame where all the connection coefficients vanish, the metric is Minkowskian, and where the proper time of the observer is equal to the Killing time. Thus, in the thin-wall approximation, one finds the effective mass per area of the two AdS_4 sides to be $2(\alpha_1 + \alpha_2)$. This positive effective mass is exactly canceled by the negative effective mass of the domain wall separating the two regions of AdS_4. Likewise, the general expression Eq. (2.43) yields a zero Tolman mass per area for the space-time.

Note that in the above calculations we have integrated along a constant time slice $-\infty < z < \infty$. As we shall see when discussing the global space-time induced from the extreme domain walls in Sec. III, there is a past and future Cauchy horizon for data placed on such a slice. The above calculation implicitly assumes no contribution to the effective mass arising from the past of the past Cauchy horizon. This assumption is consistent with the extensions of the space-time beyond the Cauchy horizon considered in Sec. III. Indeed, it is the only assumption consistent with there being a global balance of gravitational "forces."

III. GLOBAL PROPERTIES OF DOMAIN WALL SPACE-TIMES

The line elements found in the previous section are solutions to Einstein's equations under the chosen assumptions, but the global structure of the space-times they describe is not prescribed since the field equations are local. In this section we present geodesically complete space-times induced from the domain walls. In particular, we give the conformal diagrams and the corresponding coordinate atlases. As we shall see, the resulting geodesically complete space-times exhibit nontrivial causal structure. This structure is achieved without space-time singularities. The most symmetric extensions possess a lattice structure similar to those of the extreme and nonextreme Reissner-Nordström and Kerr black holes.

We begin this section with a discussion of the global space-time for the three extreme walls. Then, we present extensions for the non- and ultraextreme wall space-times. Global space-times for the non- and ultraextreme walls were described in Ref. [23] for the case with M_4 on one side and AdS_4 on the other and in Ref. [19] for the M_4–M_4 case. Here we also present the walls with AdS_4 on both sides; i.e., the non- and ultraextreme generalizations of Type II and Type III walls.[9]

As indicated earlier, the parameter β in the parametrization of the metric represents the deviation

[9]We do not discuss the global space-times of the walls with dS_4 on at least one side. Such walls can arise from quantum tunneling when $\Lambda_1 \neq \Lambda_2$ and have been discussed in Refs. [24,39–41]. The fine-tuned $\Lambda_1 = \Lambda_2 > 0$ will not be discussed here either.

of the field configuration from the corresponding supersymmetric (extreme) one. In addition, the spatial part of the metric internal to the wall ($k = \beta^2$) is geodesically complete. The curvature scalar of this part of the space-time is $2\beta^2 A(z)^{-1} S(t)^{-2}$. Therefore, only in the extreme $\beta \equiv 0$ case do we have a noncompact *planar* configuration. For $\beta \neq 0$, the walls are *compact* bubbles [19]. The (2+1)-dimensional space-time parallel to the wall is the (2+1)-dimensional de Sitter space (dS_3). The causal structure of dS_3 is similar to the well-known dS_4, which is discussed in Ref. [30]. In the following we therefore focus on the novel aspects of the direction transverse to the wall, that is, we consider geodesic extensions in the (t, z) directions.

Understanding of the space-times induced by these configurations is facilitated by examining the causal structure of pure AdS_4. For this purpose, the salient features of AdS_4 are reviewed in Appendix B.

A. Space-times of the extreme domain walls

There are three types of extreme domain walls realized [15,17] in four-dimensional ($N = 1$) supergravity theory. All these walls have $\beta \equiv 0$. Thus, they are field theoretic realizations of the planar $k = q_0 = 0$ walls. The space-time metric induced by these walls is conformally flat with conformal factor $A(z)$ becoming unity on the M_4 side of the Type I wall and falling of as $(\alpha z)^{-2}$ on the AdS_4 side, where $\Lambda = -3\alpha^2$. The Type II conformal factor falls off as $(z\alpha_{1,2})^{-2}$ on the respective sides. For the Type III wall, $A(z)$ has an irremovable coordinate singularity at a finite value of z representing the affine boundary of the space-time. In this section we present geodesically complete extensions of the space-times for Types I, II, and III extreme domain walls. The global space-times of the Type I wall have been considered previously in Ref. [18] and the Type II wall in Ref. [19].

For each of the walls, we must extend across a Cauchy horizon on the AdS_4 side [18,19]. The Cauchy horizons occur on the nulls at $|z| = \infty$ where $A(z) = 0$, i.e., where the line element degenerates. Although these nulls are an infinite proper distance away, the geodesic distance is finite. This type of geometry is familiar from the extreme black hole space-times [30–33]. The horospherical coordinates must be extended across the Cauchy horizons on these AdS_4 sides. As shown in Appendix B, the need to extend across a Cauchy horizon also arises in pure AdS_4.

Cauchy horizons represent the boundary of causal evolution; therefore, one has the possibility of making identifications across the Cauchy horizons which can introduce closed timelike curves (CTC's). The possibility of CTC's is inherited from the AdS_4 portion of the space-time. Identifications are especially intriguing for type I walls, as CTC's could lead to a supersymmetric time machine [52] for travelers leaving M_4 passing across the wall and then reemerging into the M_4 region. Due to the underlying supersymmetry, the quantum energy-momentum infinities [53–56] which plague nonsupersymmetric time machines are avoided [18,53,57].

There are three possible extensions across the null Cauchy horizons:

1. Move onto a new diamond patch with the scalar field permanently settled into its vacuum, i.e., beyond the Cauchy horizon there is pure AdS_4.
2. In the case of the Type II wall, shift the old diamond along the null such that the new diamond is oriented just as the old. This extension yields a new wall as well as a jump in the cosmological constant at the Cauchy horizon for non-Z_2 symmetric walls.[10]
3. Reflect the old diamond onto the new diamond across the Cauchy horizon. This extension leads to a new wall as well as a smooth matching of the cosmological constant at the horizon.

In the following we consider geodesic extensions of the third kind. One reason for doing so is that it yields the most interesting causal structure for the resulting space-times. It is for the third approach that the causal structure of Types I and II space-times exhibit a symmetric lattice structure similar to those first realized by the extensions of Carter for the Kerr and Reissner-Nordström black holes [32,33]. The extension for the Type I wall realizes the identical causal structure as the extreme Kerr black hole along its symmetry axis [30–32]. Finally, it is through the infinite lattice for Types I and II space-times that one eliminates the time-like boundary of pure $CAdS_4$ (the covering space of AdS_4—see Fig. 10 in Appendix B) in exchange for a countably infinite number, $\aleph_0$, of isolated points which are an infinite affine distance away from interior points (see Figs. 1 and 2). For example, the Cauchy problem for Type I space-time can be specified by prescribing initial data on one constant time slice in an AdS_4 region and freely chooosing boundary data on past null infinity of the countably infinite number of adjacent M_4 spaces (see Fig. 1). In contrast, for pure $CAdS_4$, the Cauchy problem is defined only after prescribing an infinite amount of boundary data along the timelike boundaries which has to be *self-consistent* with the specified initial data [58,59]. The third approach for the extensions can also be employed in the case of the nonextreme and ultraextreme bubbles as discussed in the next section. For this case, the infinite lattices are natural generalizations of the present extreme space-times.

The three types of extreme space-times, constructed from the third kind of geodesic extension described above, have the conformal diagrams shown in Figs. 1, 2, and 3. In each of the figures, the x and y coordinates are suppressed; therefore, each point represents an infinite plane with distances in the plane scaled by $A(z)$. The compact null coordinates $u', v' = 2\tan^{-1}[\alpha(t \mp z)]$ define the axes. As the figures indicate, these coordinates can be extended smoothly across the Cauchy horizons (denoted by the dashed nulls) separating the diamonds on the AdS_4 side. Explicitly this fact is seen by writing the (1+1)-dimensional line element near the horizon as

[10] Z_2 symmetry means $\Lambda_1 = \Lambda_2$, which can be realized for Type II walls.

$ds^2 = (\alpha z)^{-2}(dt^2 - dz^2) = \{\alpha \sin[1/2(u' - v')]\}^{-2} du' dv'$ which has a smooth extension across the null $u' = \pi, -\pi < v' < \pi$ as well as all the other Cauchy horizons. Thus, the null (u', v') coordinates provide an atlas for describing the global space-time. Note that the full (3+1)-dimensional metric has coordinate singularities in the x or y directions crossing the Cauchy horizon.

The extension chosen for the Type I wall [18] ($\sigma_{\text{ext I}} = 2\kappa^{-1}\alpha$) in Fig. 1 possesses the same causal structure as the extreme Kerr black hole along its symmetry axis [30–32]. The extension chosen for the Type II wall in Fig. 2 [$\sigma_{\text{ext II}} = 2\kappa^{-1}(\alpha_1 + \alpha_2)$] tiles the whole plane with a lattice of walls. For the Type III wall ($\sigma_{\text{ext III}} = 2\kappa^{-1}|\alpha_1 - \alpha_2|$) shown in Fig. 3, the conformal factor $A(z)$ diverges at some finite coordinate z^* [17]. This point represents the boundary of the space-time just as $z = 0$ ($\psi = \pi/2$) represents the edge of pure AdS_4 as seen in the horospherical coordinates (see Fig. 10). As a result, the extension of the Type III wall is causally the same as pure AdS_4.

For each of the extensions, the vertices are special points [19]. To illustrate their nature, consider a photon moving along one of the Cauchy horizons, say $v' = -\pi$. Since the Cauchy horizon has zero surface gravity, the

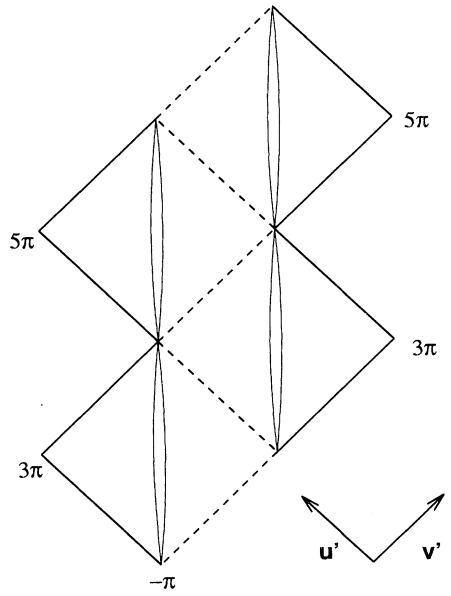

FIG. 1. Conformal diagram of the extreme Type I domain wall, which separates AdS_4 from M_4. The x and y directions are suppressed; therefore, each point represents an infinite plane with distances in the plane conformally compressed by $A(z)$. The compact null coordinates are $u', v' = 2\tan^{-1}[\alpha(t \mp z)]$. The domain wall is the double timelike arc splitting the diamonds. The complete extension consists of an infinite lattice of diamonds. The vertices are infinitely conformally compressed points; i.e., they are an infinite affine distance away from points interior. Cauchy horizons for data placed on the constant time slices in one diamond are the dashed nulls separating the AdS_4 patches. The walls smooth out the singularities at the timelike boundaries of pure AdS_4 seen in Fig. 10. The removal of the timelike boundary allows for a formulation of the Cauchy problem on the covering space-time which prescribes initial data on one slice across an AdS_4 region and freely chooses boundary data on the past null infinities of the countably infinite number of M_4 regions. Note the similarity of the extension taken here to that of the extreme Kerr black hole along its symmetry axis [30,32] (diagram taken after [18]).

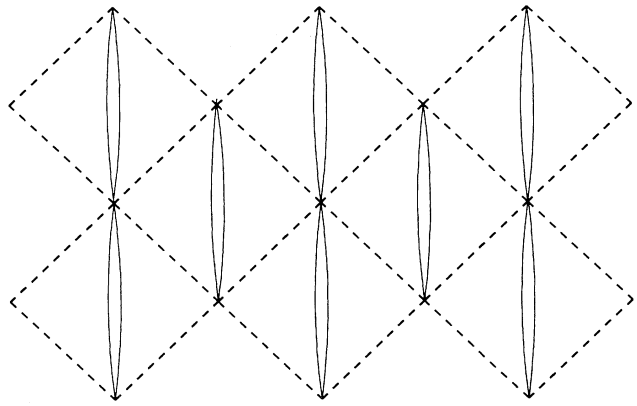

FIG. 2. Conformal diagram of the extreme Type II domain wall. Conventions follow Fig. 1. AdS_4 regions are on both sides of the wall. As there are Cauchy horizons on both sides of the wall, the geodesically complete extension covers the whole plane with an infinite lattice of domain wall diamonds.

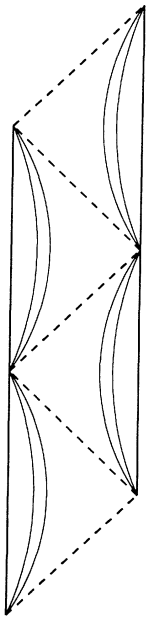

FIG. 3. Conformal diagram of the extreme Type III domain wall. Conventions follow Fig. 1. AdS_4 regions are on both sides of the domain wall. The irremovable singularity at $z = z^* = z'_-$ is represented by the timelike affine boundaries. This diagram has the same causal structure as pure AdS_4 seen in Fig. 10 (see also [20]). In this way, this system can be thought of as a generalized AdS_4.

photon never reaches the wall in the next diamond at $u' = \pi, v' = -\pi$ [60]. These points are an infinite affine distance away from all other points; i.e., they represent an infinite conformal compression. This is analogous to the situation in the extreme Reissner-Nordström and Kerr black holes [30–33].

The conformal diagram of a space-time containing a Type I or II extreme domain wall centered at $z = 0$ should be compared to that of pure AdS_4 shown in Fig. 10 in Appendix B. One sees that the timelike affine infinity of AdS_4 at $z = 0$ (equivalently $\psi = \pi/2$) is smoothed out by the wall, which allows for another space-time region across the boundary of pure AdS_4. In this sense, one can think of the wall as living at spatial infinity of AdS_4. It has been speculated [19] that the extreme walls are related to the *"Membrane at the End of the Universe"* which arises in supermembrane theory [61].

B. Space-times of nonextreme and ultraextreme domain walls

The generalizations of the extreme walls to $\beta > 0$ yield the non- and ultraextreme walls. As discussed previously, only the $k = \beta^2$ version of the line element completely covers the spherical domain wall bubble. Again, with $\sin\theta = \beta r$ in Eq. (2.13), the line element for these walls is

$$ds^2 = A(z)\left(dt^2 - dz^2 - \beta^{-2}\cosh^2\beta t\, d\Omega_2^2\right), \qquad (3.1)$$

where $d\Omega_2^2 = d\theta^2 + \sin^2\theta d\phi^2$ and $A(z)$ is given by one of the $\Lambda = 0$ and $\Lambda = -3\alpha^2$ solutions in Eq. (2.28). The $\Lambda = 3\alpha^2$ solution is not discussed here.

1. *Minkowski inside and outside of the nonextreme and ultraextreme walls*

The line element for the M_4 side of the bubble, as written in the comoving coordinates, is given by

$$ds^2 = e^{\mp 2\beta z}\left(dt^2 - dz^2 - \beta^{-2}\cosh^2\beta t\, d\Omega_2^2\right). \qquad (3.2)$$

A metric coefficient decreasing away from the wall represents the M_4 side being on the inside of the wall, and if the exponential is increasing away from it, the M_4 side is on the outside. For nonextreme walls both sides are on the inside. For ultraextreme walls, the side with the highest energy density (less negative Λ) is on the outside of the wall and the other side is on the inside. Recall that we have chosen to orient the z coordinate so that the most negative Λ term is placed on the side $z < 0$. Thus for an ultraextreme AdS_4–M_4, the M_4 side is on the outside, and it is described by the plus sign solution above, whereas for an ultraextreme M_4–dS_4, the Minkowski space is on the inside again described by the plus sign solution but now for $z < 0$.

When describing the inside, these coordinates have a cosmological horizon along the null where $|z| = \infty$. It is here that the line element (3.2) degenerates. As seen below, this horizon is a Rindler horizon arising from the hyperbolic motion of the bubble accelerating away from inertial observers. For the case of M_4 being on the outside of the bubble, the comoving coordinates are geodesically complete. The null where $z = \infty$ represents the usual affine boundary of M_4 and thus requires no extension. The two bubbles are complementary in the sense that the radii of the spatial region covered by the respective line elements, $\underline{r}^{\rm in}_{\rm out} = \beta^{-1}\exp(\mp\beta z)\cosh\beta t$, satisfy: $0 < \underline{r}^{\rm in} \le \beta^{-1}\cosh\beta t \le \underline{r}_{\rm out} < \infty$. This complementary nature is also reflected in the conformal diagrams, as we now discuss.

For the purpose of investigating the causal structure of the space-time induced by the nonextreme and ultraextreme bubbles, we introduce the radial Rindler coordinates $\underline{t}^{\rm in}_{\rm out} = \beta^{-1}\exp(\mp\beta z)\sinh\beta t$ and $\underline{r}^{\rm in}_{\rm out} = \beta^{-1}\exp(\mp\beta z)\cosh\beta t$. This transformation brings the line element Eq. (3.2) to the spherically symmetric form $ds^2 = d\underline{t}^2 - d\underline{r}^2 - \underline{r}^2 d\Omega_2^2$. The $(\underline{t}, \underline{r}, \theta, \phi)$ coordinates define an inertial frame in which the bubbles at $z = 0$ live on the hyperbolic trajectory $\underline{r}^2 - \underline{t}^2 = -\tan(u'/2)\tan(v'/2) = \beta^{-2}$. Here $u', v' = 2\tan^{-1}[\beta(\underline{t} \mp \underline{r})]$ are the usual compact null coordinates of M_4. From this hyperbolic trajectory, it is apparent that in order to remain comoving with respect to the walls, observers require a constant proper acceleration of magnitude β. Therefore, the comoving frame of the bubble is a Rindler frame [62]. The hyperbolic trajectory of the wall is a general feature of vacuum bubbles, as discussed in Refs. [3,25].

For the case where M_4 is on the inside of the bubble (e.g., the nonextreme case), the wall accelerates away from inertial observers, and consequently it produces a Rindler horizon. This horizon manifests itself as the boundary of the comoving coordinates (t, z, θ, ϕ). As this horizon arises from acceleration, freely falling particles reach it with a finite affine parameter [23]. As a result, an extension of the comoving coordinates must be provided across the horizon. As we have globally defined inertial coordinates $(\underline{t}, \underline{r}, \theta, \phi)$, the unique extension across this horizon onto pure M_4 is taken. On the outside (e.g., the M_4 side of an AdS_4–M_4 ultraextreme domain wall), the bubble accelerates toward all inertial observers and the comoving coordinates do not require an extension. Indeed, unless timelike observers maintain a constant proper acceleration not smaller than that of the bubble, the wall will eventually hit them.

The conformal diagram for the M_4 side of the nonextreme bubble is given in Fig. 4. The dotted line represents the null Rindler horizons where $|t \pm z| = \infty$. The unique extension across these horizons is into pure M_4 space-time. As seen by inertial observers in M_4, the world tube of the nonextreme bubble is represented by the surface of the (2+1)-dimensional de Sitter hyperboloid. The M_4 embedding space of dS_3 is the *physical* M_4 space for this bubble. Inertial M_4 observers are on the inside of the de Sitter hyperboloid [19]. To remain with the wall observers must accelerate toward the wall. In this global sense the wall exhibits "repulsive gravity." Figure 4 shows a slice of this hyperboloid, whose surface is the space-time trajectory of the wall. The bubble's center of symmetry is the timelike line in the center of the figure.

Opposite points represent spatially antipodal points of the sphere. The diagram has to be matched to another $q_0 = \beta^2$ solution on the wall's world tube.

In the ultraextreme AdS_4–M_4 case, the inertial M_4 observer is on the outside of the de Sitter hyperboloid. The corresponding conformal diagram (slice of the de Sitter embedding) is given in Fig. 5. Thus, the M_4 side of an AdS_4–M_4 ultraextreme wall is the complement of the nonextreme M_4 diagram of Fig. 4. Here, the nulls are the usual null infinities of pure M_4. The two hyperbolic trajectories represent the space-time trajectory of two spatially antipodal points on the wall surface. Again, the diagram is to be glued to another solution at the position of the wall, e.g., one can put the inside of the AdS_4 cylinder (described in the next section) in the hole where the de Sitter hyperboloid was taken out, and identify along the wall's trajectory.

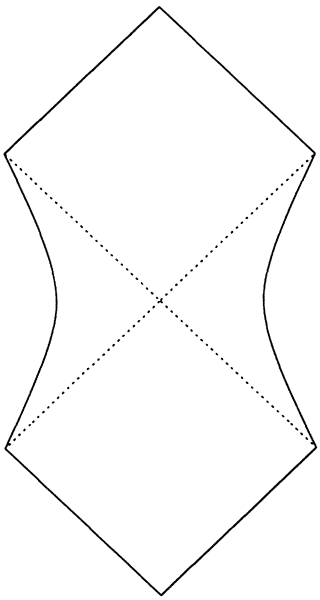

FIG. 4. Conformal diagram for the M_4 side of the nonextreme bubble or the M_4 side inside an ultraextreme bubble. This diagram is part of (3+1)-dimensional Minkowski space as seen in the compactified $(\underline{t}, \underline{r})$ plane. Angular coordinates (θ, ϕ) are suppressed. The axis of symmetry represents the world line of the center of the bubble at $\underline{r} = 0$. Opposite points on the right and left sides of $\underline{r} = 0$ represent antipodal points $\theta \to \pi - \theta$ and $\phi \to \phi + \pi$. The time direction increases upward. The solid curved lines asymptoting to the dotted nulls are the world lines of antipodal points of the nonextreme bubble wall at $z = 0$, or equivalently $\underline{r}^2 - \underline{t}^2 = -\tan(u'/2)\tan(v'/2) = \beta^{-2}$. This diagram is a cross section of the hyperboloid of dS_3 as embedded in M_4 (see [30] for the analogous case of dS_4). The rest frame of the wall is a Rindler frame whose acceleration has magnitude β. The dotted nulls are the Rindler horizons on which the comoving coordinates (t, z) degenerate ($z = \infty$). In order to remain with the wall, observers must accelerate toward it. In this sense, the nonextreme bubble exhibits "repulsive gravity." The unique extension of the comoving coordinates across the Rindler horizons is onto pure Minkowski space-time.

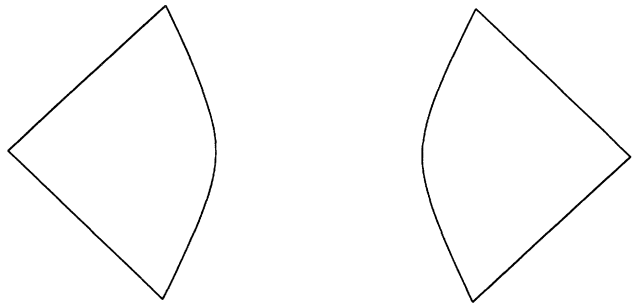

FIG. 5. Conformal diagram for the M_4 region outside of the AdS_4–M_4 ultraextreme bubble. This diagram is the complement of the nonextreme bubble of Fig. 4. The two sides represent spatially antipodal pieces of the spherically symmetric space-time. In this case, the M_4 side corresponds to the outside of the de Sitter hyperboloid of Fig. 4. These wedges are covered by the comoving coordinates (t, z). The solid curved line is the hyperbolic trajectory of the wall at $z = 0$. The solid nulls are the affine boundaries. Timelike observers with insufficient acceleration eventually encounter the wall. In this sense, the ultraextreme bubble exhibits "attractive gravity."

2. *Anti-de Sitter inside and outside of the non- and ultraextreme walls*

The line element for the AdS_4 side of the bubble, as written in the comoving coordinates, is given by

$$ds^2 = \frac{\beta^2}{[\alpha \sinh(\beta z - \beta z')]^2} \left(dt^2 - dz^2 - \beta^{-2} \cosh^2 \beta t \, d\Omega_2^2\right), \tag{3.3}$$

where $z > 0$ is the side with the less negative cosmological constant.

For the AdS_4 on the outside of an ultraextreme bubble, $z' = z'_+ > 0$, which allows $(z - z')$ to vanish at $z^* = z'_+$. z^* is an irremovable singularity in the line element and represents the timelike affine boundary of the AdS_4 side of the ultrabubble. The inside of an ultraextreme bubble has a more negative cosmological constant than the outside. This side as well as the sides with $z < 0$ of a nonextreme bubble has $z' = z'_+$, whereas the other inside of a nonextreme bubble with $z > 0$ has $z' = z'_-$, and so the line element (3.3) degenerates at $|z| = \infty$, which corresponds to the center(s) of the bubble. As with the nonextreme M_4 bubble, the null on which $|z| = \infty$ represents a cosmological horizon which is reached within a finite affine parameter by timelike and null trajectories [23]. Therefore, an extension across the horizon is necessary. This horizon arises from the compactified hyperbolic motion of the wall as viewed in the frame defined by the Einstein universe coordinates. This frame is discussed next.

The Einstein universe coordinates [30] define a frame in which the bubbles exhibit properties analogous to the M_4 side of the bubbles as seen in inertial M_4 coordinates. This frame provides the analog of the inertial frame for

the M_4 case. The transformation to the Einstein universe frame is presented in three steps. Appendix A gives the explicit form of the line element in the intermediate steps. (1) Define $\ln \Xi = \beta(z - z')$. From the definition of z', it is seen that $0 < \Xi_{\text{non}} < 1 \leq \Xi_{\text{ultra}}$. (2) Introduce the radial Rindler coordinates: $T = \Xi \sinh \beta t$ and $R = \Xi \cosh \beta t$. (3) Define the compact timelike and radial coordinates: $T \pm R = \tan[(t_c \pm \psi)/2]$. Performing these transformations on the line element (3.3) yields $ds^2 = (\alpha \cos \psi)^{-2}(dt_c^2 - d\psi^2 - \sin^2 \psi d\Omega_2^2)$, where $-\pi \leq t_c \pm \psi \leq \pi$ and $0 \leq \psi \leq \pi/2$. The spatial center of symmetry is at $\psi = R = 0$. In the frame defined by the Einstein universe coordinates, the bubble at $z = 0$ lives on a hyperbolic trajectory $R^2 - T^2 = -\tan[(t_c - \psi)/2] \tan[(t_c + \psi)/2] = e^{2\beta z'}$. To remain stationary with respect to the bubble—to stay at a fixed (z, θ, ϕ) position—requires a proper acceleration of magnitude $|a_\mu a^\mu| = \alpha^2 \cosh^2 \beta(z - z')$. Nonextreme bubbles accelerate away from observers on both sides, and thus we expect a horizon analogous to the Rindler horizon of the M_4 side. The ultraextreme bubbles approach timelike observers on the outside and eventually collide with them. The inside of an ultraextreme bubble is indistinguishable from the inside of a nonextreme bubble.

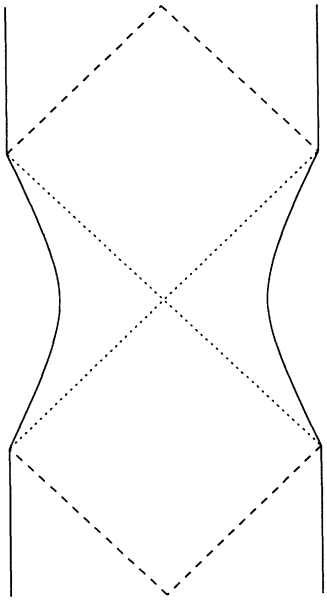

FIG. 6. Conformal diagram for an AdS_4 region inside the nonextreme or ultraextreme bubble. This diagram is part of pure AdS_4 as seen in the Einstein cylinder coordinates (t_c, ψ) (see Fig. 10). The angular coordinates (θ, ϕ) are suppressed, and the center of symmetry represents the world line of the center of the bubble at $R = \psi = 0$. The vertical boundaries are the timelike boundaries of pure AdS_4 at $\psi = \pi/2$ or $R = \infty$. Opposite points on the right and left of $\psi = 0$ represent antipodal points $\theta \to \pi - \theta$ and $\phi \to \phi + \pi$. The time direction increases upward. The solid curved lines asymptoting to the dotted nulls are the world lines of antipodal points of the nonextreme bubble wall at $z = 0$, or equivalently $R^2 - T^2 = -\tan[(t_c - \psi)/2] \tan[(t_c + \psi)/2] = \exp(2\beta z')$. The wall on the AdS_4 side sweeps out a compactified hyperbolic trajectory over half the fundamental domain of pure AdS_4 (e.g., $-\pi \leq t_c \leq 0$ in Fig. 10). The rest frame of the wall is a frame whose acceleration has magnitude $\alpha \cosh \beta(z - z')$. The dotted nulls are the horizons on which the comoving coordinates (t, z) degenerate ($z = -\infty$). The unique extension of the comoving coordinates across the horizons is onto pure AdS_4. The dashed nulls represent the Cauchy horizons of pure AdS_4.

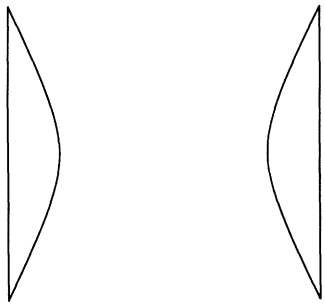

FIG. 7. Conformal diagram for the AdS_4 region outside of the ultraextreme bubble. This diagram is the complement of the nonextreme bubble in Fig. 6. Conventions are as in that figure. The comoving coordinates (t, z) cover these slivers. The vertical line is the affine boundary and the curved line is the trajectory of the bubble wall. Timelike trajectories in these patches eventually encounter the wall, just as for the M_4 ultraextreme bubble.

As seen in the Einstein cylinder coordinates, the conformal diagram for the AdS_4 inside of the non- and ultraextreme walls is shown in Fig. 6, and the AdS_4 outside of an ultraextreme wall is shown in Fig. 7. Note the complementary nature of the two diagrams; a relation also exhibited by the M_4 sides as shown in Figs. 4 and 5. For the nonextreme wall, the space-time is uniquely extended across the cosmological horizons (the dotted nulls) onto pure AdS_4 (see Appendix B). The dashed nulls are the Cauchy horizons of pure AdS_4. For the ultraextreme wall, the region between the wall at $z = 0$ and the timelike boundary of the space-time, at $z = z^* < 0$, is covered by the (t, z) coordinates.

C. Comments on the extensions

The previous conformal diagrams represent the minimal extensions of the space-times on the M_4 and AdS_4 sides of the walls. In the form presented here, they are quite similar. The difference is the presence of null affine boundaries in the M_4 regions as opposed to timelike affine boundaries in the AdS_4 regions. To obtain a complete space-time we glue the two sides together at the wall's world tube.

Since the AdS_4 inside a nonextreme bubble has a Cauchy horizon, we are able to introduce a lattice structure such as discussed in [23] and shown in Fig. 8. This lattice is a generalization of the extreme lattices shown in Figs. 1–3. The diagrams of Figs. 4–7 should be thought of as pieces of a space-time which can be fit together in different ways. In placing a wall on the AdS_4 side, we

eliminate a portion of the timelike boundary of AdS_4, and just as in the case of the extreme walls, the Cauchy problem can be formulated for the infinite lattice space-times by placing initial data on one AdS_4 slice of constant time and freely specifiable boundary data on a countably infinite ($\aleph_0$) number of past null infinities of M_4 space-times.

These lattices of walls exhibit similarities to the lattices obtained in extending the nonextreme black holes [30–32]. Furthermore, there are local coordinate relations mapping the horizons in the (time, radial) directions of the black hole space-times to the (t, z) horizons in both the extreme and nonextreme domain wall systems [18,23]. By making this coordinate connection, it is shown that near the horizons of both the nonextreme and extreme black holes (with $d\Omega = 0$), the space-times are locally AdS_2.

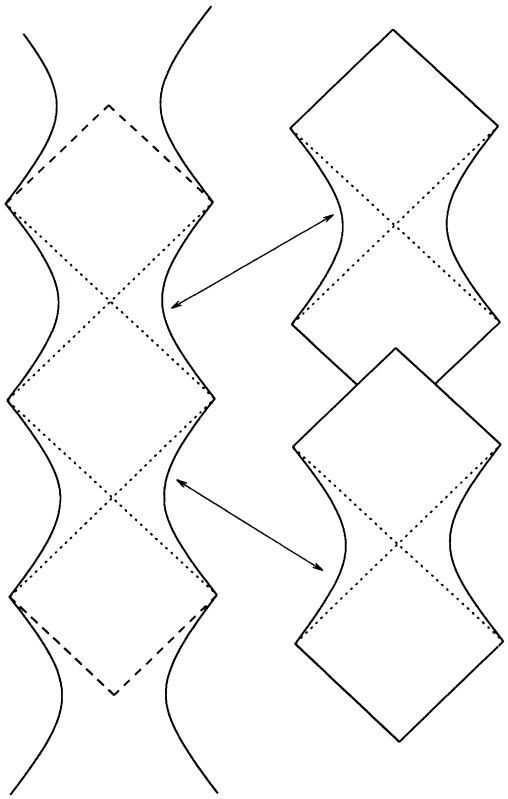

FIG. 8. Conformal diagram for the gluing together of bubble insides to form a lattice of nonextreme bubbles. The left diagram is that of the AdS_4 side shown in Fig. 6 with two successive wall trajectories asymptoting to the timelike affine boundaries. For the infinite lattice, there are an infinite number of these walls. The right diagram is that of the adjoining nonextreme M_4 bubbles shown in Fig. 4. These regions are not overlapping, i.e., they do not touch. Movement between the M_4 patches is only realized by first passing through the bubble, into the AdS_4 side, and then back out the next bubble. Periodic identifications lead to CTCs for the space-time. The two diagrams are identified across the wall region by revolving and rotating the de Sitter hyperboloid of the wall space-time as embedded in Minkowski space (the M_4 side) around the AdS_4 cylinder and identifying adjacent points of the two wall regions. In a similar manner to the extreme lattices of Figs. 1 and 2, the replacement of the timelike affine boundary allows for a more conventional Cauchy problem where initial data is placed a timelike slice across an AdS_4 region and boundary data is given on the past null infinities of the M_4 sides.

Figure 9 illustrates the causal properties of the ultra-extreme bubble corresponding to the quantum tunneling event for decay of a metastable Minkowski space-time into the lower energy anti-de Sitter vacuum. At time zero, the bounce becomes the tunneling two sphere which forms at rest with a finite radius and then accelerates along the hyperbolic Rindler trajectory. Notice that timelike trajectories on the M_4 side (the metastable side) eventually collide with the wall and pass through into the AdS_4 region (the stable side). This situation was addressed by Coleman and De Luccia [25] and later by Abbott and Coleman [63] who used a singularity theorem of Penrose [64] to conclude that a bubble of AdS_4 forming inside an M_4 region is unstable to the formation of singularities. A necessary assumption for establishing this result is the absence of Cauchy horizons. In this regard, the dashed null in Fig. 9 is drawn to indicate the Cauchy horizon for data placed on any constant time slice after the bubble forms. The existence of this horizon precludes the use of Penrose's theorem for establishing the singularity result.

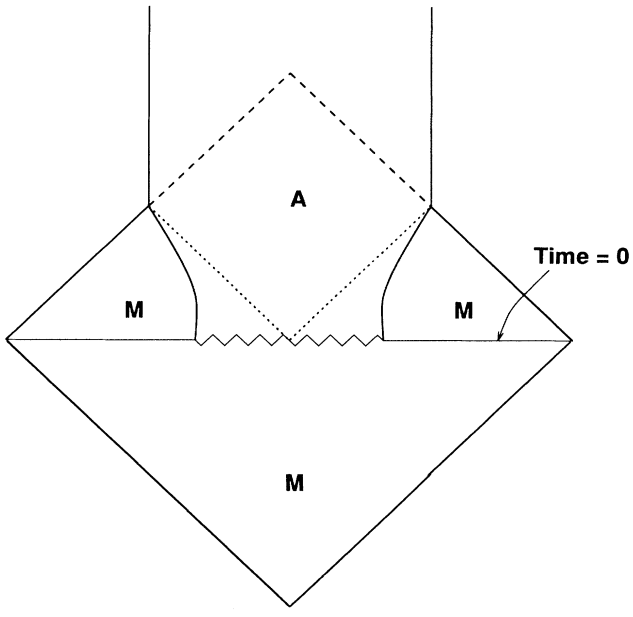

FIG. 9. Conformal diagram for the classical evolution of a quantum tunneling event where M_4 (**M**) decays into AdS_4 (**A**). This is the ultraextreme bubble where M_4 is outside and the lower cosmological constant (and thus higher pressure) AdS_4 region is inside. The gluing of the diagrams is performed as in Fig. 8. The quantum tunneling bubble forms at real time $(t = \underline{t} = t_c)$ = imaginary time = zero. The tunneling event cannot be described by classical gravity, thus the jagged line in this region.

IV. DISCUSSION

We have studied the space-times of vacuum domain walls in general relativity interpolating between vacua of nonequal cosmological constant. Our emphasis has been on vacua of nonpositive cosmological constant since the resulting solutions are the natural generalizations of the supersymmetric walls studied in Refs. [15–19]. The coordinates in which the domain wall is spatially at rest (the comoving coordinates) is a useful frame for deducing the local properties of the solutions through the use of Israel's formalism of singular hypersurfaces. We have presented a unified picture of three types of domain walls: (1) extreme (supersymmetric) walls which are static, noncompact planar configurations, with surface energy density $\sigma = \sigma_{\rm ext}$; (2) nonextreme domain walls which are bubbles with two insides and energy density $\sigma = \sigma_{\rm non} > \sigma_{\rm ext}$; and (3) the ultraextreme walls which correspond to the false vacuum decay bubbles with energy density $\sigma = \sigma_{\rm ultra} < \sigma_{\rm ext}$.

A. Domain walls as gravitational shields

The extreme AdS_4–M_4 space-time (Type I) represents a solution where the gravitationally repulsive domain wall exactly compensates the gravitational attraction caused by the negative energy AdS_4 vacuum. This precise balancing is realized with the added feature of an increased symmetry in the field equations, i.e., the configuration is supersymmetric and is described by first-order rather than second-order equations. One could say that the Type I domain wall acts as a gravitational shield protecting M_4 observers from the curved space-time of the AdS_4 side.

Upon breaking supersymmetry, the energy density of the wall can increase or decrease. Additionally, the noncompact planar geometry of the wall is replaced by a compact spherical bubble with time dependent radius. Increasing the energy of the wall, one may expect to get a bubble where the repulsive domain wall overcompensates the attractive gravity of the AdS_4 region inside the bubble. If this were the case, the result would be a finite object with negative effective gravitational mass. Negative mass objects introduce very interesting possibilities [10]. For example, controlling such objects would allow for a free source of acceleration [11]. This fact can be seen through the equivalence principle, which implies that the negative mass object falls toward any positive mass, which in turn is repelled by the negative mass object. Note that this propulsion mechanism does not violate conservation of momentum since the negative mass object has a momentum vector antiparallel to its velocity. The present analysis has, however, shown that for the domain walls considered, space-time is warped so that observers on both sides of the would-be negative mass object (the nonextreme bubble) are on the inside of the bubble. Hence, this kind of negative mass object *cannot* be observed from the outside.

As noted above, these classes of solutions shed light on the nature of configurations with negative effective gravitational mass. They indicate a new kind of censorship, analogous to Penrose's cosmic-censorship hypothesis [65,66]. Nature does not only keep singularities hidden under horizons, but also seems to prevent us from being outside negative mass objects. Accordingly, the supersymmetric type I wall system represents the lowest gravitational energy state accessible to an outside observer in Minkowski space. When the energy density of the domain wall is further increased, thus decreasing the effective gravitational mass below zero, the bubble curves onto both sides making both sides of the bubble an *inside*. We conjecture that similar protection will take place in all singularity free models and formulate:

The Positive Mass Conjecture: *There is no singularity free solution of Einstein's field equations for physically acceptable matter sources for which an exterior observer can see a finite object with a negative effective gravitational mass.*

By "physically acceptable" we mean that matter sources—not including the vacuum itself—obey the weak energy condition, and "singularity free" does not exclude singular hypersurfaces tractable by Israel's formalism.

At the same time we see see that supersymmetry serves as a *positive mass protector* in the sense that supersymmetry is characteristic of the limiting case where the total effective gravitational mass is zero below which the domain wall encloses space on both sides. Again, we note the analogy with cosmic censorship where supersymmetry has been identified as a cosmic censor [27].

B. Relation to physical domain walls

In this paper we have presented the local and global properties of exact solutions of Einstein's field equations for infinitely thin walls. To obtain them it was necessary to assume a high degree of symmetry. Yet, however idealized these solutions may be, many of the properties of these solutions are shared by more realistic, physical domain walls.

Cosmological domain walls are the transition region between two different vacua and there are at least three ways of forming walls in a cosmological context: (1) Walls separating vacua that are absolutely stable against quantum tunneling could form via the Kibble mechanism [1,2]. (2) Primordial walls which could be born with the universe when it was created by a quantum tunneling process out of nothing [4–6]. This tunneling can yield regions of different vacuum states separated by walls. (3) Walls could also be the boundary of a bubble created from a first-order phase transition between a false and true vacuum through the mechanism of quantum tunneling [3,25].

The stable vacuum manifold for a scalar field theory consists of minima of the scalar potential which are not connected by quantum tunneling. For scalar theories without gravity, any potential possessing minima of the same energy are degenerate; there is no tunneling because the corresponding bounce instanton has infinite action [3]. Conversely, if there is a nonzero difference in the value of the scalar energy at the minima, there will be a

finite probability for decay to the global minima through the formation of a tunneling bubble [3,67–69]. In the case with gravity, the coupling of a constant scalar vacuum energy to gravity through the *effective* cosmological constant, the value, and most importantly the *sign,* of the vacuum energy are essential for understanding the stability of a vacuum to quantum decay.

For dS_4, gravity always tends to increase the probability for decay to a lower cosmological constant vacuum relative to the corresponding process in the nongravitational theory [25]. Therefore, the domain walls considered in Sec. II separating different cosmological constant vacua, where at least one vacuum is dS_4, represent the local properties for the classical evolution of a bubble formed from such a first-order phase transition. Discussions of these bubbles can be found in the literature [24,39–41]. Only those walls separating dS_4 of the *same* cosmological constant are stable topological walls, and these are unstable to perturbations in the adjacent vacuum energy.

If one vacuum is M_4 and the other AdS_4 [25], or if both vacua are AdS_4 [21], there is a lowering of the probability for decay relative to the corresponding nongravitational case. If the scalar potential energy barrier is such that the surface energy of the tunneling bubble $\sigma_{\rm bubble}$ is greater than or equal to $2\kappa^{-1}(\alpha_1+\alpha_2)$, where $\Lambda_1=-3\alpha_1^2$ and $\Lambda_2=-3\alpha_2^2$, then the tunneling instanton has infinite action which renders the tunneling probability to zero. As a result, stable topological domain walls can exist between such vacua even without the scalar energy in the two vacua being the same.

We have discussed three kinds of walls: the nonextreme, extreme, and ultraextreme walls. Here we point out the relation between the idealized models and physical domain walls. The nonextreme wall, whose surface energy is $\sigma_{\rm non} > 2\kappa^{-1}(\alpha_1+\alpha_2)$, correspond to walls which may have formed by the Kibble mechanism or to primordial domain walls born with the universe at the time of creation. If one starts out with a universe with closed spatial sections, and allows the scalar field to fall into two different vacua, these two regions can be separated by a nonextreme bubble with two insides. A lower dimensional picture will illustrate that this can happen. Assume that we live in a two-dimensional space, represented by the surface of a sphere. Let us divide it in two halves along a great circle. Both sides are on the inside of the great circle. Therefore, if the initial spatial geometry is closed, the seemingly strange topology of the nonextreme wall causes no problem to the creation of walls of this type through the Kibble mechanism. Indeed, it has been speculated [24,40] that we actually live inside a nonextreme bubble.

The ultraextreme wall, whose surface energy is $\sigma_{\rm ultra} < 2\kappa^{-1}(\alpha_1+\alpha_2)$, represents the classical evolution of a quantum tunneling bubble (which also could be primordial) that forms when a metastable region of Minkowski or anti-de Sitter false vacuum decays into a lower energy anti-de Sitter vacuum. First-order phase transitions of this type can occur in theories for which the potential energy barrier is insufficient to suppress the tunneling.

There is no tunneling [21] between supersymmetric vacua since the minimal energy tunneling bubble saturates the Coleman-De Luccia bound: $\sigma_{\rm bubble}=2\kappa^{-1}(\alpha_1+\alpha_2)$, thus rendering the decay probability to zero. This result is exact to all orders in Newton's constant and applies to both supersymmetric AdS_4–AdS_4 and AdS_4–M_4 vacua. As a consequence, all supersymmetric vacua are degenerate in the sense that there is no tunneling between them. The noncompact planar extreme walls with surface tension $\tau=\sigma_{\rm wall}=2\kappa^{-1}(\alpha_1+\alpha_2)$ interpolate between these supersymmetric vacua [15–17]. The extreme walls separate supersymmetric vacua of nonpositive cosmological constant where at least one of the vacua is anti-de Sitter and they are the configurations intermediate to the spherical non- and ultraextreme bubbles.

C. Final remarks

We have given a unified, global presentation of the gravitational aspects of domain walls. Apart from the theoretical insight in general relativity and supersymmetry gained from these walls, and the relation to possible physical realizations of domain walls in Nature, we also would like to point out the didactic value of these solutions. In this very simple model one encounters maximally symmetric spaces, Tolman's mass, Israel's thin wall formalism, comoving coordinates and the FLRW metric, the de Sitter hyperboloid, Rindler motion, cosmological horizons, Cauchy horizons, and the problem of geodesic incompleteness. For this reason, it is an ideal tool for illustrating many important concepts and techniques in general relativity.

The role of the supersymmetric domain wall as a perfectly balanced planar configuration *intermediate* between two types of spherically symmetric bubbles have been explained. For wall energy densities below the supersymmetric value (ultraextreme), the wall surface curves away from timelike observers on the side with the highest vacuum energy density and accelerates toward them. If the wall energy density is above the supersymmetric value (nonextreme), the wall curves toward observers on both sides and accelerates away from them. Analysis of these nonextreme bubbles has also yielded the "positive mass conjecture," which precludes the free acceleration realized from gravitating bodies of negative effective mass. We also note that supersymmetry serves as a "positive mass protector."

This study has provided the first steps toward a theoretical foundation for studying the cosmological effects of these walls; especially those arising from supergravity where the vacua are either supersymmetric or have spontaneously broken supersymmetry. It should, however, be emphasized that physically realistic domain walls break many of our symmetry assumptions by being wiggly and anisotropic.

To conclude, the domain wall solutions give valuable insight in nonperturbative aspects of gravity. In particular, it is noteworthy that gravity, however weak it might be, determines the topology of the domain walls. In this way, nonperturbative gravitational effects play a very important role both in the evolution of cosmic domain walls

and in the evolution of the inside of quantum tunneling bubbles.

ACKNOWLEDGMENTS

We would like to thank J. Garriga, A. D. Linde, P. J. Steinhardt, and A. Vilenkin for discussions. H. H. Soleng would like to thank Professor Paul J. Steinhardt for the invitation to spend the sabbatical year 1992–93 at the University of Pennsylvania, and he would like to express his gratitude to the Department of Physics for its hospitality. This work was supported in part by U.S. DOE Grant No. DOE-EY-76-C-02-3071, NATO Research Grant No. 900-700 (M. C.), Fridtjof Nansen Foundation Grant No. 152/92 (H. H. S.), Lise and Arnfinn Heje's Foundation Ref. No. 0F0377/92 (H. H. S.), and by the Norwegian Research Council for Science and the Humanities (NAVF), Grant No. 420.92/022 (H. H. S.).

APPENDIX A: COORDINATE TRANSFORMATIONS

In this paper we produced a number of line elements describing vacuum solutions external to domain walls. In this appendix we provide local transformations relating the coordinates natural for the wall geometry to canonical coordinates for the appropriate vacuum solutions. We present results only for the cases $q_0 = 0,\ +\beta^2$, since the case $q_0 = -\beta^2$ corresponds to a solution with a metric that is singular for certain proper times.

1. *Extremal walls ($q_0 = 0$)*

The $k = 0$ solutions are written in the canonical static coordinates: Cartesian for M_4 and horospherical for AdS_4. The horospherical coordinates are discussed in Refs. [19,20].

The $k = -\beta^2$ line elements are related to the $k = 0$ line elements through a coordinate transformation not involving the spatial coordinate z. For this case, consider the metric for flat (2+1)-dimensional space-time written in planar polar coordinates

$$ds^2 = d\underline{t}^2 - d\underline{r}^2 - \underline{r}^2 d\phi^2. \tag{A1}$$

Introducing the Milne coordinates [43,62]

$$\underline{t} = t\cosh\beta\chi, \quad \underline{r} = t\sinh\beta\chi, \tag{A2}$$

brings the line element to

$$ds^2 = dt^2 - (\beta t)^2\left[d\chi^2 + \beta^{-2}\sinh^2\beta\chi\, d\phi^2\right]. \tag{A3}$$

Transforming to a radial coordinate $r = \beta^{-1}\sinh\beta\chi$ yields

$$ds^2 = dt^2 - (\beta t)^2\left(\frac{dr^2}{1+(\beta r)^2} + r^2 d\phi^2\right). \tag{A4}$$

Finally, addding an extra dimension coordinated by z and allowing for a nonpositive cosmological constant yields

$$ds^2 = A(z)\left[dt^2 - dz^2 - (\beta t)^2\left(\frac{dr^2}{1+(\beta r)^2} + r^2 d\phi^2\right)\right], \tag{A5}$$

where $A(z)$ is one of the $q_0 = 0$ (extremal) solutions in Eqs. (2.27).

2. *Non- and ultraextreme walls ($q_0 = \beta^2$)*

a. The $\Lambda = -3\alpha^2$ solution. Consider the AdS_4 metric as written in the Einstein universe coordinates discussed in Appendix B:

$$ds^2 = (\alpha\cos\psi)^{-2}\left(dt_c^2 - d\psi^2 - \sin^2\psi\, d\Omega_2^2\right). \tag{A6}$$

Note that these coordinates, just as the Schwarzschild-coordinates, cover the whole AdS_4 manifold. In the latter coordinates the metric is

$$\alpha^2 ds^2 = \left(1+\rho^2\right)dt_c^2 - \left(1+\rho^2\right)^{-1}d\rho^2 - \rho^2 d\Omega_2^2, \tag{A7}$$

where $\rho = \tan\psi$. We now decompactify the coordinates (t_c, ψ) by introducing

$$T \pm R = \tan[\tfrac{1}{2}(t_c \pm \psi)]. \tag{A8}$$

This transformation, restricted to the branch $-\pi \le t_c \pm\psi \le \pi$, brings the line element (A6) to

$$ds^2 = \frac{4}{\alpha^2(T^2 - R^2 + 1)^2}\left(dT^2 - dR^2 - R^2 d\Omega_2^2\right). \tag{A9}$$

Transforming to the *radial* Rindler coordinates [62] $T = e^{\beta(z-z')}\sinh\beta t$ and $R = e^{\beta(z-z')}\cosh\beta t$, where z' is given in Eq. (2.30), brings (A9) to

$$ds^2 = \frac{\beta^2}{\left[\alpha\sinh(\beta z - \beta z')\right]^2}\left(dt^2 - dz^2 - \beta^{-2}\cosh^2\beta t\, d\Omega_2^2\right). \tag{A10}$$

This metric corresponds to the first of the solutions of Eq. (2.28).

b. The $\Lambda = 0$ solution. Starting from the flat space-time metric written in spherical coordinates,

$$ds^2 = d\underline{t}^2 - d\underline{r}^2 - \underline{r}^2 d\Omega_2^2, \tag{A11}$$

and transforming to the *radial* Rindler coordinates [62]

$$\underline{t} = \beta^{-1}e^{\pm\beta z}\sinh\beta t, \quad \underline{r} = \beta^{-1}e^{\pm\beta z}\cosh\beta t, \tag{A12}$$

brings the line element to the desired form

$$ds^2 = e^{\pm 2\beta z}\left(dt^2 - dz^2 - \beta^{-2}\cosh^2\beta t\, d\Omega_2^2\right). \tag{A13}$$

This metric corresponds to the second of the solutions (2.28).

c. The $\Lambda = 3\alpha^2$ solution. Starting from the de Sitter

metric in canonical coordinates

$$ds^2 = d\overline{T}^2 - \cosh^2\alpha\overline{T}\left(\frac{d\rho^2}{1-\alpha^2\rho^2} + \rho^2 d\Omega_2^2\right) \quad \text{(A14)}$$

and defining $(\cos t_c)^{-1} \equiv \cosh\alpha\overline{T}$ and $\sin\psi \equiv \alpha\rho$ gives the metric

$$ds^2 = \frac{1}{\alpha^2\cos^2 t_c}\left(dt_c^2 - d\psi^2 - \sin^2\psi\, d\Omega_2^2\right). \quad \text{(A15)}$$

We now decompactify the coordinates (t_c, ψ) by defining T and R as in Eq. (A8). This transformation restricted to $-\pi \le t_c \pm \psi \le \pi$, brings the de Sitter metric (A14) to the form

$$ds^2 = \frac{4}{\alpha^2(T^2 - R^2 - 1)^2}\left(dT^2 - dR^2 - R^2 d\Omega_2^2\right). \quad \text{(A16)}$$

Transforming to the Rindler coordinates $T = e^{\beta(z-z'')}\sinh\beta t$ and $R = e^{\beta(z-z'')}\cosh\beta t$, where z'' is given in Eq. (2.31), brings (A16) to

$$ds^2 = \frac{\beta^2}{[\alpha\cosh(\beta z - \beta z''))]^2}\left(dt^2 - dz^2 - \beta^{-2}\cosh^2\beta t\, d\Omega_2^2\right). \quad \text{(A17)}$$

This metric corresponds to the third of the solutions in Eq. (2.28).

APPENDIX B: ASPECTS OF ADS

To help in understanding the properties of space-times with a domain wall where at least one side is AdS_4, we present here the salient features of AdS_4. More detailed discussions of AdS_4 can be found in Hawking and Ellis [30], Avis *et al.* [58], Gibbons [19], and Griffies [20].

1. *AdS*$_4$

AdS_4 is the maximally symmetric solution to Einstein gravity in four space-time dimensions with a negative cosmological constant $\Lambda \equiv -3\alpha^2$

$$\mathcal{R}_{\mu\nu} - \tfrac{1}{2}\mathcal{R}g_{\mu\nu} = -3\alpha^2 g_{\mu\nu}. \quad \text{(B1)}$$

The length scale of AdS is set by its "radius" α^{-1}.

AdS_4 is isomorphic to the coset $SO(3,2)/SO(3,1)$ and is realized as a hyperboloid embedded in a flat five-dimensional space with *two* timelike directions: $\eta_{AB}Y^AY^B = \alpha^{-2}$ and $\eta_{AB} = \mathrm{diag}(+1,-1,-1,-1,+1)$. One can completely cover the hyperboloid and thus all of AdS_4 with the following choice of *spherical* or *Einstein universe* coordinates:

$$\begin{aligned}
\alpha Y^0 &= \cos t_c \sec\psi,\\
\alpha Y^1 &= \sin\theta\cos\phi\tan\psi,\\
\alpha Y^2 &= \sin\theta\sin\phi\tan\psi,\\
\alpha Y^3 &= \cos\theta\tan\psi,\\
\alpha Y^4 &= -\sin t_c\sec\psi.
\end{aligned} \quad \text{(B2)}$$

The line element $ds^2 = \eta_{AB}dY^AdY^B$ takes on the form

$$ds^2 = (\alpha\cos\psi)^{-2}\left(dt_c^2 - d\psi^2 - \sin^2\psi\, d\Omega_2^2\right), \quad \text{(B3)}$$

and the range on these dimensionless coordinates sufficient to cover all of AdS_4 is $-\pi \le t_c \le \pi$, $0 \le \psi < \pi/2$, $0 \le \theta \le \pi$, $0 \le \phi < 2\pi$. The line element without the $(\alpha\cos\psi)^{-2}$ conformal factor is that of the static Einstein universe, where in addition $0 \le \psi \le \pi$. The spherical coordinates are inextendable; i.e., all geodesic motion on AdS_4 is described in these coordinates.

AdS_4 has the topology $\mathbf{S}^1(\text{time})\times\mathbf{R}^3(\text{space})$ which means it has a periodic time and closed timelike curves (CTC's). This fact is intimately related to the negative vacuum energy density (negative cosmological constant) which violates the familiar positive energy conditions. In the context of Type II walls, Gibbons discusses this point in Ref. [19]. If satisfied, these energy conditions restrict space-times to have a nonperiodic timelike coordinate. It is possible to avoid CTC's by using the covering space-time $CAdS_4$ in which the compact time coordinate t_c is allowed to range over the whole real line. In other words, we unwrap the $\mathbf{S}^1(\text{time})$ rendering the topology $\mathbf{R}^4$. Nevertheless, neither $CAdS_4$ nor AdS_4 have a Cauchy surface, and on account of this, neither AdS_4 nor $CAdS_4$

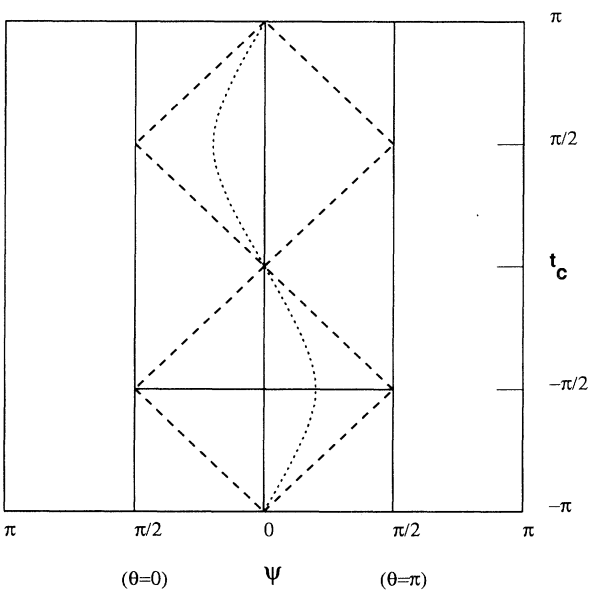

FIG. 10. AdS_4 as seen on the Einstein cylinder. AdS_4 is the region $0 \le \psi \le \pi/2$ and $-\pi \le t_c < \pi$. The covering space-time, $CAdS_4$, is the region $-\infty < t_c < \infty$. The static Einstein universe is the region $0 \le \psi \le \pi$ and $-\infty < t_c < \infty$. Timelike and null world lines are indicated. The 45° dashed lines which form the diamonds are the null geodesics. The dotted periodic lines are the timelike geodesics. For increasing energy, the timelike geodesics approach the nulls and thus reach closer to affine infinity located at $\psi = \pi/2$. Left of the center is identified with $\theta = 0$ and the right with $\theta = \pi$. Data place on the constant time slices, say $t_c = -\pi/2$, have past and future Cauchy horizons given by the dashed nulls forming the diamonds. In the horospherical coordinates with line element $ds^2 = (\alpha z)^{-2}(dt^2 - dx^2 - dy^2 - dz^2)$, the affine boundary at $\psi = \pi/2$ maps to $z = 0$ [17,19,20] (figure taken after Avis, Isham, and Storey [58]).

is globally hyperbolic. Therefore, an infinite amount of boundary data as well as initial data must be introduced in order to properly define the Cauchy problem [58,59]. AdS_4 can be regarded as the canonical space-time in which the issues of Cauchy horizons and CTCs arise.

2. *AdS_4 mapped on the Einstein universe*

In understanding the global aspects of AdS_4, such as its causal and geodesic properties, it is useful to map AdS_4 onto the Einstein cylinder. The static Einstein universe has the topology $\mathbf{R}(\text{time})\times\mathbf{S}^3(\text{space})$ and the line element

$$ds_c^2 = dt_c^2 - d\psi^2 - \sin^2\psi\, d\Omega_2^2 = dt_c^2 - d\Omega_3^2 \qquad \text{(B4)}$$

where $-\infty < t_c < \infty$, $0 \le \psi, \theta \le \pi$, $0 \le \phi < 2\pi$. $CAdS_4$ is conformal to the half of the static Einstein universe with $0 \le \psi < \pi/2$. If we suppress the S^2 coordinates θ and ϕ, the Einstein universe is a cylinder with ψ running along the $\mathbf{S}^1$ and t_c along the $\mathbf{R}$. Since $0 \le \psi < \pi$, opposite sides of the cylinder are identified. Cutting the cylinder at $\psi = \pi$ yields Fig. 10. AdS_4 is the region where $0 \le \psi < \pi/2$, $-\pi \le t_c \le \pi$ and each point on the cylinder a two-sphere $\mathbf{S}^2$ of radius $\alpha^{-1}\tan\psi$. Radial nulls are at 45°. The nontrivial causal structure of AdS_d, where $d \ge 2$, is understood from investigating AdS_2.

3. *Geodesic structure of AdS_2 as seen on the Einstein cylinder*

Integration of the geodesic equations on AdS_d is facilitated by the maximal symmetry of the space-time. For AdS_4, maximal symmetry allows us to lay down coordinates such that the geodesic of interest has zero θ and ϕ angular momentum. The geodesics are thus determined by the AdS_2 line element

$$ds^2 = (\alpha\cos\psi)^{-2}\left(dt_c^2 - d\psi^2\right). \qquad \text{(B5)}$$

Introducing the conserved energy parameter[11] $E = (\alpha\cos\psi)^{-2}dt_c/d\tau$, where τ is the affine parameter (proper time for the timelike geodesics), allows us to express the line element for these geodesics $ds^2 = d\tau^2 > 0$ as

$$(d\psi/d\tau)^2 = (\alpha\cos\psi)^4\left[E^2 - (\cos\psi)^{-2}\right]. \qquad \text{(B6)}$$

Note that the timelike nature of the motion imposes the constraint $(\alpha E)^2 \ge 1$. Solving for $\psi(\tau)$ and $t_c(\tau)$ is straightforward. Eliminating τ yields the periodic world line for the timelike test particles

$$\sin^2\psi = \left[1 - (\alpha E)^{-2}\right]\sin^2 t_c. \qquad \text{(B7)}$$

Setting E to infinity in (B7), yields the null world line

$$\sin^2\psi = \sin^2 t_c. \qquad \text{(B8)}$$

Finite energy timelike geodesics never reach $\psi = \pi/2$. Rather, the constant curvature of AdS_4 acts as a perfect gravitational harmonic oscillator causing the timelike test particles to always return to their original position in a proper time of π/α. Thus, the proper time period for a full transit through a fundamental AdS_4 domain is $2\pi/\alpha$. This oscillatory motion is consistent with AdS_4 having the positive gravitational mass density of $6\kappa^{-1}\alpha^2$ at every point; cf. Eq. (2.45). These world lines are indicated in Fig. 10.

4. *Cauchy horizon for AdS_2*

As can be seen from obtaining the null geodesics in terms of the null affine parameter [20], nulls reach $\psi = \pi/2$ only after an infinite affine parameter. This means that $\psi = \pi/2$ is identified as the affine boundary of AdS_d. It is here that the line element (B3) has an irremovable coordinate singularity which is characteristic of affine boundaries. The timelike nature of $\psi = \pi/2$ precludes AdS_4 from having a Cauchy surface. Space-times with a Cauchy surface allow for a deterministic description of the classical evolution of free fields given a sufficient amount of initial data placed on a spacelike slice [30]. Equivalently, every point to the future of a Cauchy surface must have a past directed light-cone which intersects it. It follows that a Cauchy surface cannot be timelike. Since spatial infinity in AdS_4 is timelike, information evolved from some initial spacelike slice, say $t_c = -\pi$ in Fig. 10, can be corrupted from data flowing in from beyond the null diamonds. These nulls represent the Cauchy horizon for this data.

[11] The mass dimension of E is -1.

[1] T. W. B. Kibble, Phys. Rep. **67**, 183 (1980).
[2] For a review, see, e.g., A. Vilenkin, Phys. Rep. **121**, 263 (1985).
[3] For a review, see, e.g., S. Coleman, *Aspects of Symmetry* (Cambridge University Press, Cambridge, England, 1985).
[4] A. Vilenkin, Phys. Lett. **117B**, 25 (1982); Phys. Rev. D **30**, 509 (1984).
[5] J. B. Hartle and S. W. Hawking, Phys. Rev. D **28**, 2960 (1983).
[6] A. D. Linde, Nuovo Cimento Lett. **39**, 401 (1984).
[7] R. C. Tolman, Phys. Rev. **35**, 875 (1930).
[8] See, e.g., Ø. Grøn, Am. J. Phys. **54**, 46 (1986).
[9] J. Ipser and P. Sikivie, Phys. Rev. D **30**, 712 (1984).
[10] For a discussion of the amusing properties of negative mass particles, see R. H. Price, Am. J. Phys. **61**, 216 (1993).
[11] A. P. Lightman, W. H. Press, R. H. Price, and S. A. Teukolsky, *Problem Book in Relativity and Gravitation* (Princeton University Press, Princeton, New Jersey,

1975), Prob. 13.20.
[12] W. B. Bonnor, Gen. Relativ. Gravit. **21**, 1143 (1989).
[13] A. D. Dolgov and I. B. Khriplovich, Gen. Relativ. Gravit. **21**, 13 (1989).
[14] B. Linet, Int. J. Theor. Phys. **34**, 1159 (1985).
[15] M. Cvetič, S. Griffies, and S.-J. Rey, Nucl. Phys. **B381**, 301 (1992).
[16] For a review, see M. Cvetič and S. Griffies, in *Proceedings of the International Symposium on Black Holes, Membranes and Wormholes,* The Woodlands, Texas, 1992, edited by S. Kalara and D. Nanopoulos (World Scientific, Singapore, in press).
[17] M. Cvetič and S. Griffies, Phys. Lett. B **285**, 27 (1992).
[18] M. Cvetič, R. L. Davis, S. Griffies, and H. H. Soleng, Phys. Rev. Lett. **70**, 1191 (1993).
[19] G. W. Gibbons, Nucl. Phys. **B394**, 3 (1993).
[20] S. Griffies, Ph.D. thesis, University of Pennsylvania, Philadelphia, 1993.
[21] M. Cvetič, S. Griffies, and S.-J. Rey, Nucl. Phys. **B389**, 3 (1993).
[22] R. Brustein and P. J. Steinhardt, Phys. Lett. B **302**, 196 (1993).
[23] M. Cvetič, S. Griffies, and H. H. Soleng, Phys. Rev. Lett. **71**, 670 (1993).
[24] V. A. Berezin, V. A. Kuzmin, and I. I. Tkachev, Phys. Lett. **120B**, 91 (1983).
[25] S. Coleman and F. De Luccia, Phys. Rev. D **21**, 3305 (1980).
[26] G. W. Gibbons, in *Supersymmetry, Supergravity and Related Topics,* Proceedings of the XVth GIFT International Seminar on Theoretical Physics, Sant Feliv de Guixols, Girana, Spain, 1984, edited by F. del Aguila *et al.* (World Scientific, Singapore, 1985).
[27] R. E. Kallosh, A. D. Linde, T. M. Ortín, A. W. Peet, and A. van Proeyen, Phys. Rev. D **46**, 5278 (1992).
[28] E. Mach, *Die Mechanik in Ihrer Entwicklung Historisch-Kritisch Dargestellt* (1883), *The Science of Mechanics* 6th ed., translated by T. J. McCormack (Open Court, LaSalle, Illinois, 1960).
[29] Ø. Grøn and E. Eriksen, Gen. Relativ. Gravit. **21**, 105 (1989).
[30] S. W. Hawking and G. F. R. Ellis, *The Large Scale Structure of Space-Time* (Cambridge University Press, Cambridge, England, 1973).
[31] S. Chandrasekhar, *The Mathematical Theory of Black Holes* (Oxford University Press, New York, 1983).
[32] B. Carter, Phys. Rev. **141**, 1242 (1966).
[33] B. Carter, Phys. Lett. **21**, 423 (1966).
[34] W. Israel, Nuovo Cimento **44B**, 1 (1966); **48B**, 463(E) (1967).
[35] For a generalization of the Israel formalism [34] to lightlike shells, see C. Barrabès and W. Israel, Phys. Rev. D **43**, 1129 (1991).
[36] See, e.g., C. W. Misner, K. S. Thorne, and J. A. Wheeler, *Gravitation* (Freeman, San Francisco, 1973).
[37] S. Weinberg, *Gravitation and Cosmology: Principles and Applications of the General Theory of Relativity* (Wiley, New York, 1972).
[38] K. Tomita, Phys. Lett. **162B**, 287 (1985).
[39] H. Sato, Prog. Theor. Phys. **76**, 1250 (1986).
[40] S. K. Blau, E. I. Guendelman, and A. H. Guth, Phys. Rev. D **35**, 1747 (1987).
[41] V. A. Berezin, V. A. Kuzmin, and I. I. Tkachev, Phys. Rev. D **36**, 2919 (1987).
[42] Ø. Grøn and H. H. Soleng, Phys. Lett. A **165**, 191 (1992).
[43] H. P. Robertson and T. W. Noonan, *Relativity and Cosmology* (Saunders, Philadelphia, PA, 1968).
[44] G. W. Gibbons and C. M. Hull, Phys. Lett. **109B**, 190 (1982).
[45] A. Vilenkin, Phys. Lett. **133B**, 177 (1983).
[46] G. Goetz, J. Math. Phys. **31**, 2683 (1990).
[47] M. Mukherjee, Class. Quantum Grav. **10**, 131 (1993).
[48] D. A. Macdonald, R. H. Price, W.-M. Suen, and K. S. Thorne, in *Black Holes: The Membrane Paradigm,* edited by K. S. Thorne, R. H. Price, and D. A. Macdonald (Yale University Press, New Haven, 1986).
[49] Ø. Grøn, Phys. Rev. D **31**, 2129 (1985).
[50] H. H. Soleng, "Inverse Square Law of Gravitation in (2+1)-Dimensional Space-Time as a Consequence of Casimir Energy," University of Pennsylvania Report No. UPR-0540-T, 1992 (unpublished).
[51] P. A. Amundsen and Ø. Grøn, Phys. Rev. D **27**, 1731 (1983).
[52] Time machines are also realized in wormhole models, see, e.g., J. Friedman, M. S. Morris, I. D. Novikov, F. Echeverria, G. Klinkhammer, K. S. Thorne, and U. Yurtsever, Phys. Rev. D **42**, 1915 (1990).
[53] S. W. Hawking, Phys. Rev. D **46**, 603 (1992).
[54] G. Klinkhammer, Phys. Rev. D **46**, 3388 (1992).
[55] M. Visser, Phys. Rev. D **47**, 554 (1993).
[56] J. D. E. Grant, Phys. Rev. D **47**, 2388 (1993).
[57] C. P. Burgess, Nucl. Phys. **B259**, 473 (1985).
[58] S. J. Avis, C. J. Isham, and D. Storey, Phys. Rev. D **18**, 3565 (1978).
[59] P. Breitenlohner and D. Z. Freedman, Ann. Phys. (N.Y.) **144**, 249 (1982).
[60] R. H. Boyers, Proc. R. Soc. London **A311**, 245 (1969).
[61] E. Bergshoeff, M. J. Duff, C. N. Pope, and E. Sezgin, Phys. Lett. B **199**, 69 (1987); **224**, 71 (1989).
[62] N. D. Birrell and P. C. W. Davies, *Quantum Fields in Curved Space* (Cambridge University Press, Cambridge, England, 1982).
[63] L. F. Abbott and S. Coleman, Nucl. Phys. **B259**, 170 (1985).
[64] R. Penrose, Phys. Rev. Lett. **14**, 57 (1965).
[65] R. Penrose, Riv. Nuovo Cimento **1**, 252 (1969).
[66] R. Penrose, Ann. N.Y. Acad. Sci. **224**, 125 (1973).
[67] P. H. Frampton, Phys. Rev. Lett. **37**, 1378 (1976).
[68] S. Coleman, Phys. Rev. D **15**, 2929 (1977); **16**, 1248(E) (1977).
[69] C. G. Callan and S. Coleman, Phys. Rev. D **16**, 1762 (1977).